Chem Soc Rev

Catalytic Fast Pyrolysis of Lignocellulosic Biomass

Catalytic Fast Pyrolysis of Lignocellulosic Biomass

Changjun Liu[1], Huamin Wang[2], Ayman M. Karim[2], Junming Sun[1], Yong Wang[1,2*]

[1] The Gene and Linda Voiland School of Chemical Engineering and Bioengineering, Washington State University, Pullman, WA 99164, United States
[2] Institute for Integrated Catalysis, Pacific Northwest National Laboratory, Richland, WA 99352, United States

*corresponding author: wang42@wsu.edu

Abstract:

Increasing energy demand, especially in the transportation sector, and soaring CO_2 emissions necessitate the exploitation of renewable sources of energy. Despite the large variety of new energy carriers, liquid hydrocarbon still appears to be the most attractive and feasible form of transportation fuel with considerations of energy density, stability and existing infrastructure. Biomass is an abundant, renewable source of energy; however, utilizing it in a cost-effective way is still a substantial challenge. Lignocellulose is composed of three major biopolymers, namely cellulose, hemicellulose and lignin. Fast pyrolysis of biomass is praised as an efficient and feasible process to selectively convert lignocellulose into a liquid fuel—bio-oil. However bio-oil from fast pyrolysis contains a large amount of oxygen, distributed in hundreds of oxygenates. These oxygenates lead to many negative properties, such as low higher heating value, high corrosiveness, high viscosity, and instability; they also greatly limit the application of bio-oil particularly as transportation fuels. Hydrocarbons derived from biomass are most attractive because of their high energy density and compatibility with existing infrastructure. Thus, converting lignocellulose into transportation fuels via catalytic fast pyrolysis has attracted much attention. Many works related to catalytic fast pyrolysis of biomass have been published. The main challenge of this process is the development of active and stable catalysts that can deal with a large variety of decomposition intermediates from lignocellulose. This review starts with the current understanding of the chemistry in fast pyrolysis of lignocellulose and focuses on the development of catalysts in catalytic fast pyrolysis. Recent progress in the experimental studies on catalytic fast pyrolysis of biomass is also summarized with the emphasis on bio-oil yields and quality.

Keywords: catalyst, catalytic fast pyrolysis, lignocellulosic biomass, zeolite, mesoporous material

1. Introduction

The world total primary energy supply and consumption in 2010 was double that in 1971, as was CO_2 emission.[1] The worldwide delivered energy consumption is projected to increase

continuously in the next two decades with an average annual growth of about 1.6% (Table D1in the reference).[2] Despite the large variety of new energy carriers, liquid hydrocarbon still appears to be the most attractive and feasible form of transportation fuel, including aviation fuel.[3] The U.S. renewable fuels standard (RFS2) requires increasing the domestic supply of alternative fuels to 36 billion gallons by 2022, including 15 billion gallons from corn-based ethanol and 21 billion gallons of advanced biofuels from lignocellulosic biomass. The U.S. Energy Information Administration projects that the production of liquid fuels from biomass will soar in the next 30 years whether oil prices are low or high (Figure 59 in the reference).[4] New technologies must be developed for the efficient conversion of biomass to fuels that have high energy density and compatibility with existing energy infrastructure.[5]

Lignocellulosic biomass (such as wood, grass, and agricultural waste) is the most abundant and cheapest carbon source and therefore has been identified as scalable, economically viable, and potentially carbon neutral feedstock for the production of renewable biofuels via appropriate technologies. Biochemical conversion methodologies proposed for lignocelluloses await cost-effective technologies[6] and can only process cellulosic and hemicellulosic portions of lignocellulosic biomass. However, the thermochemical conversion routes are more energy efficient,[7] and more flexible in terms of feed and products.[8] Among the primary thermochemical conversion routes (i.e., gasification, and fast pyrolysis), fast pyrolysis is the most economically feasible way to convert biomass into liquid fuels,[6] and therefore has attracted a great deal of research over the past two decades. A techno-economic analysis of three conversion platforms (i.e., pyrolysis, gasification, and biochemical) comparing capital and operating cost for near-term biomass-to-liquid fuels technology scenarios was performed recently. The analysis showed that the stand-alone biomass-to-liquid fuel plants are expected to produce fuels with a product value in the range of $2.00–5.50 per gallon gasoline equivalent, with fast pyrolysis the lowest, and bio-chemical the highest.[6] Fast pyrolysis shows the highest yield to liquid fuel products and retains most of the energy from feedstocks in the liquid products.[9-11] Biomass conversion via fast pyrolysis is also on the verge of commercialization.[12] For instance, Envergent (a joint venture between UOP/Honeywell and Ensyn) has a pilot-scale demonstration plant under construction in Hawaii for biomass conversion to fuels via fast pyrolysis.[13]

The primary liquid product of fast pyrolysis of biomass is generally called bio-oil, which is obtained by immediately quenching the pyrolysis vapors. Bio-oils are composed of a large variety of condensable chemicals derived from many simultaneous and sequential reactions during the pyrolysis of lignocellulosic biomass. Bio-oil is a highly complex mixture of more than 300 oxygenated compounds.[10, 14, 15] As shown in   Such a distribution also influences the physical properties of bio-oil.

Table 1, typical bio-oil from fast pyrolysis of woody biomass has high oxygen content and low H/C ratio compared to crude oil. The chemical composition classified by functional groups with relative abundance is shown in Figure 1. The main components include three major families of compounds: (i) small carbonyl compounds such as acetic acid, acetaldehyde, acetone, hydroxyaldehydes, hydroxyketones, and carboxylic acids; (ii) sugar-derived compounds such as furfural, levoglucosan, anhydrosugars, furan/pyran ring-containing compounds; and (iii) lignin-derived compounds, which are mainly phenols and guaiacols; oligomers of a molecular weight ranging from 900 to 2500 are also found in significant amounts.[16-18] The distribution of

these compounds mostly depends on the type of biomass used and the process severity.[14, 18-22] Such a distribution also influences the physical properties of bio-oil.

Table 1 Typical elementary composition of bio-oil and crude oil. (Adapted with permission from Dickerson et al., *Energies*, 2013, **6**, 514-538. [20] Copyright 2013 MDPI)

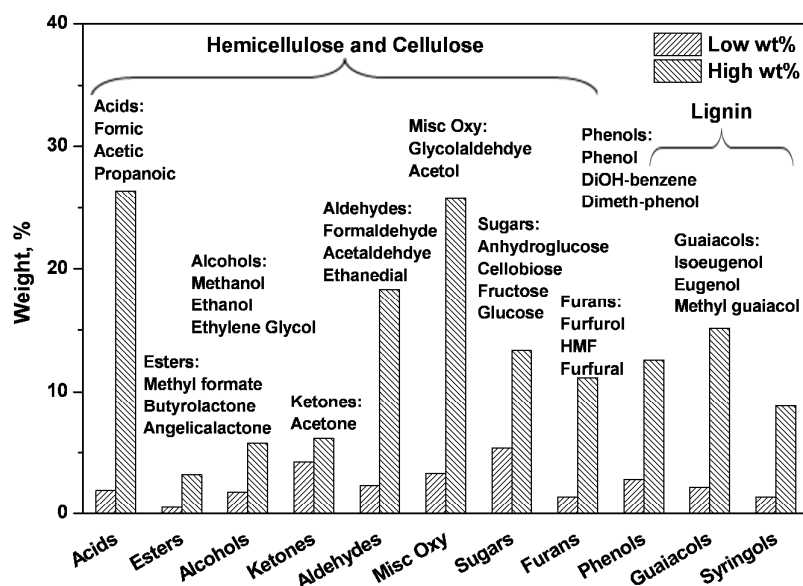| Composition	Bio-oil	Crude oil
Water (wt%)	15–30	0.1
pH	2.8–3.8	—
Density (kg/L)	1.05–1.25	0.86–0.94
Viscosity 50°C (cP)	40–100	180
HHV (MJ/kg)	16–19	44
C (wt%)	55–65	83.86
O (wt%)	28–40	<1
H (wt%)	5–7	11–14
S (wt%)	<0.05	<4
N (wt%)	<0.4	<1
Ash (wt%)	<0.2	0.1
H/C	0.9–1.5	1.5–2.0
O/C	0.3–0.5	~0

Figure 1 Chemical composition of bio-oil from wood biomass and the most abundant molecules of each of the components (Adapted with permission from Huber et al., *Chem. Rev.*, 2006, **106**, 4044-4098.[23] Copyright 2006 American Chemical Society).

Some properties of bio-oil from fast pyrolysis of lignocellulosic biomass significantly limit its direct utilization as transportation fuels in current systems. Generally, bio-oils are characterized by low vapor pressure, low heating value, high acidity, high viscosity, and high reactivity.[18, 19, 23] Bio-oils show a wide range of boiling temperatures due to their complex compositions. These adverse characteristics, particularly the instability of bio-oil, are associated with the high oxygen content in the bio-oil, which is considered a primary issue among the differences between bio-oils

and hydrocarbon fuels.[18, 24] The low heating value and flame temperature, greater ignition delay, and lower combustion rate of bio-oil are largely due to the high water content (15–30 wt%), although water could reduce the viscosity and enhance the fluidity.[18, 25] The low pH of 2–3 of bio-oil is due to the significant amount of carboxylic acids, mainly formic and acetic acids (Figure 1), and leads to its corrosiveness to common construction materials such as carbon steel and aluminum as well as some sealing materials.[18] The high content of acidic components also makes the bio-oils extremely unstable. The physicochemical properties of bio-oils change as a function of time under ordinary storage conditions.[26] The viscosity of bio-oil increases due to secondary condensation and polymerization of the high concentration of reactive components like aldehydes, ketones, and phenols.[27] In distillation, 35–50 wt% of the primary bio-oil is left as residue due to the polymerization of reactive components and the substantial amounts of nonvolatile sugars and oligomeric phenols. Highly oxygenated bio-oils are immiscible with hydrocarbon fuels, which hinders their use as fuel additives.

It is desirable and necessary to improve the quality of bio-oil toward properties similar to those of hydrocarbon fuel by certain upgrading techniques.[28-30] Oxygen must be removed before the bio-oil can be used as a replacement for diesel and gasoline.[10, 23] Bio-oil can be upgraded either off-line or during the fast pyrolysis assisted with a catalyst, the so-called catalytic fast pyrolysis (CFP). Both cases require catalysts to efficiently remove oxygen. Till now, catalytic deoxygenation has been extensively investigated for more than three decades and generally includes two approaches: catalytic cracking and hydrotreating.[31-33] Catalytic cracking creates products of lower oxygen content than the feed by solid acid catalysts such as zeolites at atmospheric pressure without the requirement of hydrogen. However, the process produces low grade products (benzene, toluene, and small chain alkanes), which requires further refining, and has low carbon yield because of significant coke formation, which results in a very short catalyst lifetime.[34] Hydrotreating of bio-oil adopts the conventional fuel hydrotreating technologies and gives desired products by removing oxygen by hydrodeoxygenation and breaking the larger molecules in the presence of pressurized hydrogen atmosphere and a catalyst such as supported molybdenum sulfide.[35, 36] Bio-oil hydrotreating has been well developed and produces high grade product. There are excellent reviews that have summarized the historical developments[35], recent advances,[36] and new focuses on hydrogeoxygenation of lignin-derived bio oils[37, 38]. However, because of the bio-oil instability and high oxygen content, hydrotreating suffers from high operating cost associated with significant catalyst deactivation, expensive catalysts used, and substantial hydrogen consumption. [39]

An alternative way is to use a catalyst to directly upgrade the pyrolysis vapors prior to quenching to produce bio-oil with improved quality, a process that is called catalytic fast pyrolysis (CFP). By instantly treating the hot pyrolysis vapor with the proper catalyst, the pyrolysis intermediates are simultaneously cracked/upgraded into hydrocarbons as the biomass is pyrolyzed.[5] The catalyst could be either directly mixed with biomass feedstock or only mixed with the pyrolysis vapors. The process where the catalyst is mixed directly with the feedstock in the pyrolysis reactor is referred to as *in situ* catalytic fast pyrolysis (*in situ* CFP)[40] while the process where the catalysts are only contacted with the pyrolysis vapors is referred to as *ex situ* catalytic fast pyrolysis (*ex situ* CFP).[40] CFP has great potential to produce hydrocarbons directly from biomass or produce higher quality bio-oils with improved stability lending them more amenable for the subsequent upgrading process. The obvious advantage of CFP is the simplified process and

avoided condensation and re-evaporation of the pyrolysis oil,[41] since it is impossible to evaporate the bio-oils completely without degrading once they have been condensed.[18, 42] The pyrolysis reaction pathways could be the same for both catalytic and non-catalytic fast pyrolysis of biomass since the bulk physical mixing of biomass and catalyst will not be able to lead to molecular level interaction. However, the presence of catalyst could promote the secondary reactions of pyrolysis intermediates toward certain products, and therefore considerably improve the conversion and selectivity to desirable components in the produced bio-oil.[43] It is known that bio-oil produced by fast pyrolysis is a highly oxygenated mixture of carbonyls, carboxyls, phenolics, and water.[44] In CFP, hydrocarbons are formed by removing oxygen from the pyrolysis-vapor intermediates in the form of CO_2, CO, and H_2O. The CFP process will lead to stabilized products and reduce the hydrogen demand in the necessary hydrotreating process that follows. The removal of the most active oxygenates, such as carbonyl- and carboxyl-containing components, in CFP could also stabilize primary bio-oils which are less prone to coke deposition and in turn improves the carbon yield to the final fuel products and long-term stability of the upgrading process.[35, 45] CFP also provides the possibility of process intensification by means of multi-scale integration and coupling of the reactions and reaction heats, which reduce processing cost. Many factors affect the performance and economic feasibility of CFP of biomass. Catalysts, heating rate, residence time, and reaction temperature are the four pivotal factors. The atmosphere in the reactor is also critical.[43, 46] As Lin and Huber pointed out how critical the catalysis is in lignocellulosic biomass conversion[47], a suitable catalyst is the key to a successful CFP process.[48] For instance, aromatic carbon yields as high as 30% was achieved by catalytic fast pyrolysis of glucose on ZSM-5,[49] and this number can be further increased to 40% on Ga/ZSM-5.[50] Recently, Rezaei et al. reviewed the catalytic cracking of oxygenate compounds derived from biomass pyrolysis with the emphasis on aromatic selectivity and olefin selectivity using zeolite catalysts.[51]

CFP has attracted increasing attention in recent years, and numerous studies have been reported over a variety of catalysts regarding the fundamental and practical aspects of CFP. Few recent reviews have focused on CFP[20, 52] and other more general reviews have also highlighted the importance of CFP.[12, 43, 53] This review will start with the pyrolysis mechanism of lignocellulose and mainly focus on the recent advances on catalyst development for CFP and related fundamental understanding of the reaction mechanisms/routes in CFP for the sake of future catalyst exploration and design.

2. Fast pyrolysis chemistry

Fundamental understanding of the chemical properties of lignocellulosic biomass and the chemistry of the reactions taking place during the fast pyrolysis and CFP is essential to rationally design more effective process and catalyst for fast pyrolysis and CFP. In this section, we will summarize the recent advancement on the chemistry of lignocellulosic biomass, the fast pyrolysis of major composition of lignocellulosic biomass, and the catalytic fast pyrolysis of lignocellulosic biomass.

Lignocellulosic biomass is a complex material, mainly composed of cellulose, hemicellulose, and lignin in addition to extractives (tannins, fatty acids, resins) and inorganic salts.[54-57] The content of each component varies with the type of biomass; the woody biomass typically contains about 40–47 wt% cellulose, 25–35 wt% hemicellulose, and about 16–31 wt% lignin.[19, 58] Cellulose is a linear polymer of glucose connected by β-1,4-glycoside linkage, which forms the framework of the biomass cell walls.[54] Cellulose is the most important element in biomass and has both

crystalline and amorphous forms.[59] Most of them are highly crystalline in nature with the polymeric degree frequently in excess of 9000.[60, 61] . Hemicellulose is structurally amorphous and possesses a heterogeneous composition. It is formed by copolymers of five different C_5 and C_6 sugars, namely glucose, galactose, mannose, xylose, and arabinose.[60] Unlike cellulose, hemicellulose is soluble in dilute alkali and consists of branched structures that vary considerably among biomass resources.[62] Lignin is a complex three-dimensional polymer of propyl-phenol groups bound together by ether and carbon-carbon bonds. The three basic phenol-containing components of lignin are *p*-coumaryl/*p*-hydroxylphenyl, coniferyl/guaiacyl, and sinapyl/syringlyl alcohol units. They are linked with C-O (β-O-4, α-O-4, 4-O-5 linking style) and C-C (β-5, 5-5, β-1, β-β linking style) bonds.[63]

2.1. Chemistry of non-catalytic fast pyrolysis of lignocellulosic biomass

2.1.1. Fast pyrolysis process

Fast pyrolysis of lignocellulose proceeds by rapid heating of biomass to moderate temperature in the absence of oxygen and immediate quenching of the emerging pyrolysis vapors. Pyrolysis products are separated into char, gases, and bio-oil. Table 2 compares the process conditions and product distribution of three different pyrolysis techniques. Fast pyrolysis gives the highest yield to bio-oil. Pyrolysis temperature, heating rate, residence time, and particle size all are important operation parameters affecting bio-oil production. The optimum pyrolysis temperature was found to be about 500°C.[64] Residence time greatly affects the secondary reactions of pyrolysis vapors. Increasing residence time could either increase the gas phase cracking or the secondary decomposition of pyrolysis vapors on the char surface. Those secondary reactions could take place either inside or outside the biomass particles. The intra-particle vapor-solid interactions are particularly important for large size particles (>0.5 cm). Thus biomass particle size < 2 mm has been recommended for maximum bio-oil yield.[54, 64]

Table 2 Comparison of three pyrolysis techniques

Pyrolysis Technology	Process Conditions			Products		
	Residence time	Heating rate	Temperature	Char	Bio-oil	Gases
Conventional	5–30 min	< 50°C/min	400–600°C	<35%	<30%	<40%
Fast Pyrolysis	<5 sec	~1000°C/s	400–600°C	<25%	<75%	<20%
Flash Pyrolysis	<0.1 sec	~1000°C/s	650–900°C	<20%	<20%	<70%

Earlier efforts to understand the fundamentals of thermal pyrolysis of lignocellulose were mainly focused on the global kinetic modeling development using thermogravimetric and differential scanning calorimetry techniques with products and intermediates lumped according to the phase and molecular weight.[65-68] The conversion was defined by the weight loss while the products were lumped into char, tar, and gases. The thermal decomposition behavior of the three main components of lignocellulose, namely, cellulose[43, 69-77], hemicellulose,[77-81] and lignin,[43, 77, 82-91] were investigated to decouple the complexity in both chemistry and kinetic models. Generally the three main components were assumed to decompose independently, and volatiles are evolved from cellulose and hemicellulose while char is mainly from lignin.[92, 93] In most of the reports, process parameters such as particle size, heating rate, and pyrolysis temperature were discussed and optimized to achieve high liquid yields. Here we mainly focus on the development of understanding the chemistry and molecular products of pyrolysis. In thermogravimetric analysis (TGA) studies, it was found that pyrolysis of hemicellulose and cellulose occurred quickly.[14, 62, 65,

[77] Hemicellulose mainly decomposed at 220−315°C, and cellulose decomposed mainly at 315−400°C (Figure 2). However, lignin is more difficult to decompose and the weight loss occurred in a wide temperature range (160−900°C) with high solid residue generation (Figure 2).[65, 77] Next, we will further summarize the chemistry of the reaction occurring during pyrolysis of the individual component in lignocellulose.
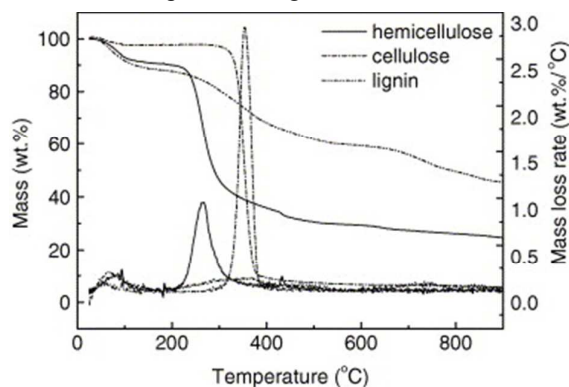

Figure 2 Pyrolysis curves of hemicellulose, cellulose, and lignin from TGA. (Adapted with permission from Yang et al., *Fuel*, 2007, **86**, 1781-1788.[77] Copyright 2007 Elsevier)

2.1.2. Fast pyrolysis of cellulose

Cellulose is the most extensively studied component in lignocellulose due to its abundance and the simplicity of its structure. The degree of crystallinity and the dimensions of the crystallites are the most important properties related to the stability and reactivity of cellulose. Each repeating unit of cellulose has three hydroxyl groups; those hydroxyl groups form either intramolecular or intermolecular hydrogen bonds, which is highly relevant to the single-chain conformation and stiffness. The intermolecular hydrogen bonding in cellulose is responsible for the sheet-like nature of the native polymer.[58]

Cellulose, together with cellobiose, α-cyclodextrin, glucose, and levoglucosan, are widely employed in mechanism studies of cellulose fast pyrolysis.[73, 74, 94-98] Free radical mechanisms,[75, 99, 100] concerted mechanisms,[94, 101-104] and ionic mechanisms[105, 106] have been proposed for cellulose pyrolysis. Cellulose transforms to a liquid before its degradation and then decomposes in two pathways. One directly leads to certain small molecular products such as furan, levoglucosan, glycoalaldehyde, and hydroxyl acetone[70, 74], while the other pathway forms low-degree oligomers. The low-degree oligomers can further break down to form furan, light oxygenates, char, permanent gases, and levoglucosan (Figure 3).[67, 107] 27 compounds including char have been identified by GC-MS analysis of pyrolyzed cellulose and its surrogates .[74] The major products are levoglucosan, hydroxyacetaldehyde, furfural, formic acid, acetic acid, and aldehyde compounds.[54, 74, 108, 109]

Initially, levoglucosan is generated in its liquid form in cellulose pyrolysis and then some of it volatilizes to be a primary volatile product of. It can also undergo condensed-phase secondary pyrolysis to form pyrans and light oxygenates (Figure 4).[69, 74, 107, 110, 111] Various small linear oxygenates have been formed from gradual decomposition of levoglucosan.[73, 94, 112] It is interesting that levoglucosan itself is relatively stable and does not break down when pyrolyzed alone.[67, 113] The secondary decomposition of levoglucosan was found induced by the pyrolysis vapors from cellulose and lignin and inhibited by the xylan-derived vapor.[98] Dehydration and

7

isomerization of levoglucosan lead to the formation of other anhydro-monosaccharides. These anhydro-monosaccharides may either re-polymerize to form anhydro-oligomers or further transform to smaller oxygenates by fragmentation/retro-aldol condensation, dehydration, decarbonylation, or decarboxylation.[69]

Char is obviously an undesired product in CFP. The secondary reaction of primary pyrolysis products was found to increase the char yield.[95, 114] Re-polymerization and secondary pyrolysis of levoglucosan was found to be an important pathway for char formation.[111, 113] Increasing the residence time of volatiles results in higher char yield due to the higher degree of secondary reaction of the primary pyrolysis products.[114]
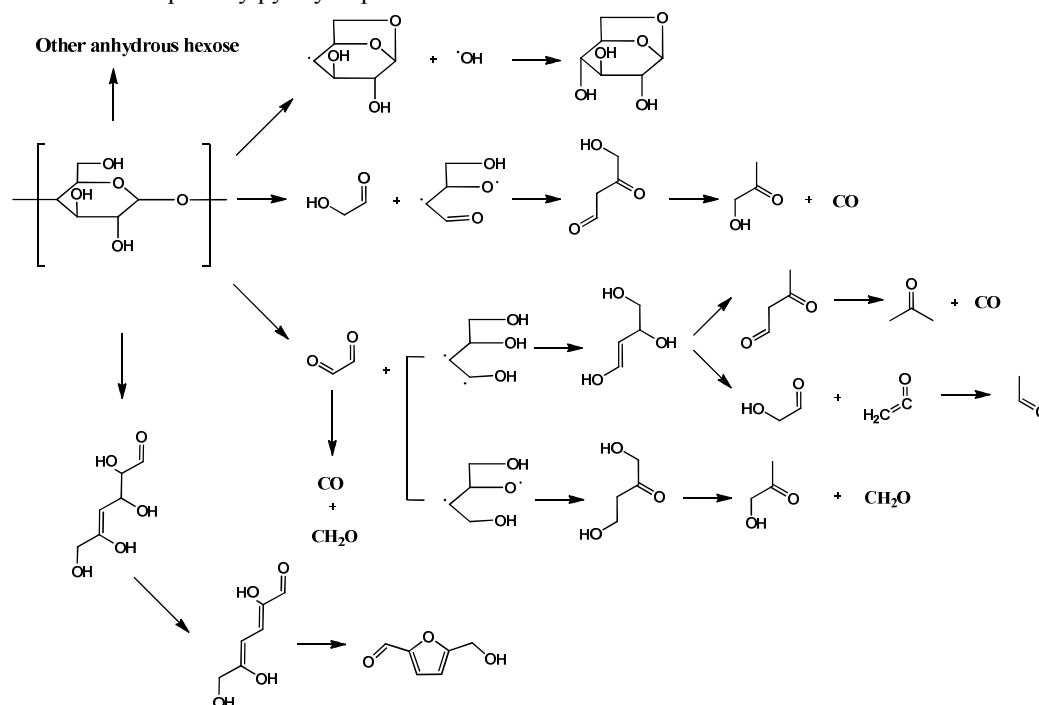

Figure 3 Reaction pathways for the direct decomposition of cellulose molecules. (Adapted with permission from Shen et al., *Bioresour. Technol.*, 2009, **100**, 6496-6504.[75] Copyright 2009 Elsevier)
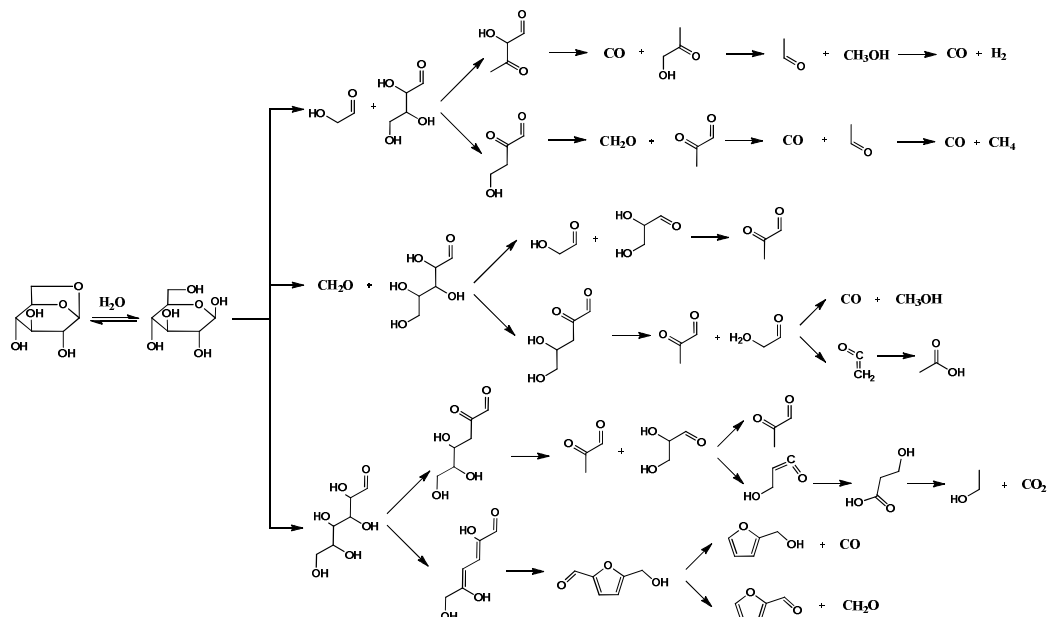
Figure 4 Reaction pathways for secondary decomposition of anhydrosugars (especially levoglucosan). (Adapted with permission from Shen et al., *Bioresour. Technol.*, 2009, **100**, 6496-6504.[75] Copyright 2009 Elsevier)

2.1.3. Fast pyrolysis of hemicellulose

Hemicellulose is complex polysaccharide usually with general formula $(C_5H_8O_4)_m$ and polymerization degree of 50−200.[62] Xylan is the most abundant hemicellulose; it widely exists in woody biomass.[115] Commercially available xylan has often been used as a surrogate for hemicellulose.[78] Hemicellulose is more readily decomposed than cellulose in thermal pyrolysis (Figure 2).[77] Fast pyrolysis of hemicellulose is also speculated to proceed by a radical mechanism.[80] Similar to the pyrolysis of cellulose, small oxygenates are formed either competitively or consequentially from fast pyrolysis of hemicellulose (Figure 5).[78] Water, methanol, formic, acetic, propionic acids, hydroxyl-1-propanone, hydroxyl-1-butanone, 2-methylfuran, 2-furfuraldehyde, dianhydroxylopyranose, and anhydroxylopyranose are identified as the main products.[78, 116] The production of dianhydro xylopyranose—a double dehydration product of xylose was explained by the lack of a sixth carbon and a substituted oxygen at the fourth position which helps to stabilize the primary pyrolysis product by forming a single dehydration product.[78, 117] Thus the xylosyl cation formed from pyrolysis undergoes subsequent glycosidic bond cleavage and dehydration, which forms dianhydro xylopyranose. Xylose could be formed while the xylosyl cations react with H^+ and OH^- in its vicinity.
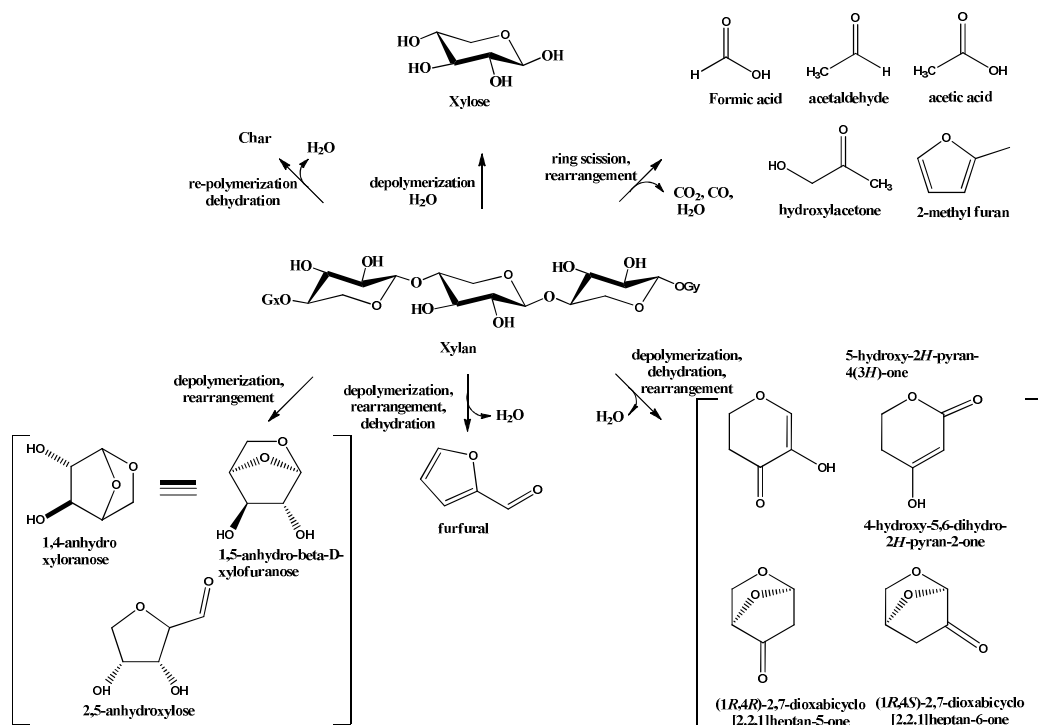
Figure 5 Proposed reaction scheme of hemicellulose pyrolysis. (Adapted with permission from Patwardhan et al., *ChemSusChem*, 2011, **4**, 636-643.[78] Copyright 2011 John Wiley and Sons)

2.1.4. Fast pyrolysis of lignin

Lignin is an important cell-wall component of biomass, especially woody species. Recently Laskar et al. and Saidi et al. reviewed the pathway for lignin conversion with the focus on lignin isolation and catalytic hydrodeoxygenation of lignin-derived bio-oils.[37, 38] The three basic structural units of lignin are *p*-coumaryl alcohol, coniferyl alcohol, and sinapyl alcohol. The relative abundances of *p*-coumaryl alcohol, coniferyl alcohol, and sinapyl alcohol units vary with the sources of biomass but the linkages (Figure 6 Common phenylpropane linkages in lignin. (Adapted with permission from Chakar et al., *Ind. Crop and Prod.*, 2004, **20**(2), 131-141.[121] Copyright 2004Elsevier)) are similar.[62, 118-120] Among all the interphenylpropane linkages involved in lignin substructures, the guaiacylglycerol β-aryl ether substructure is the most abundant (40–60%). The abundances of other substructures found in lignin macromolecules are phenyl coumarone (10%), diarylpropane (5–10%), pinoresinol (5% or less), biphenyl (5–10%), and diphenyl ether (5%).[62]
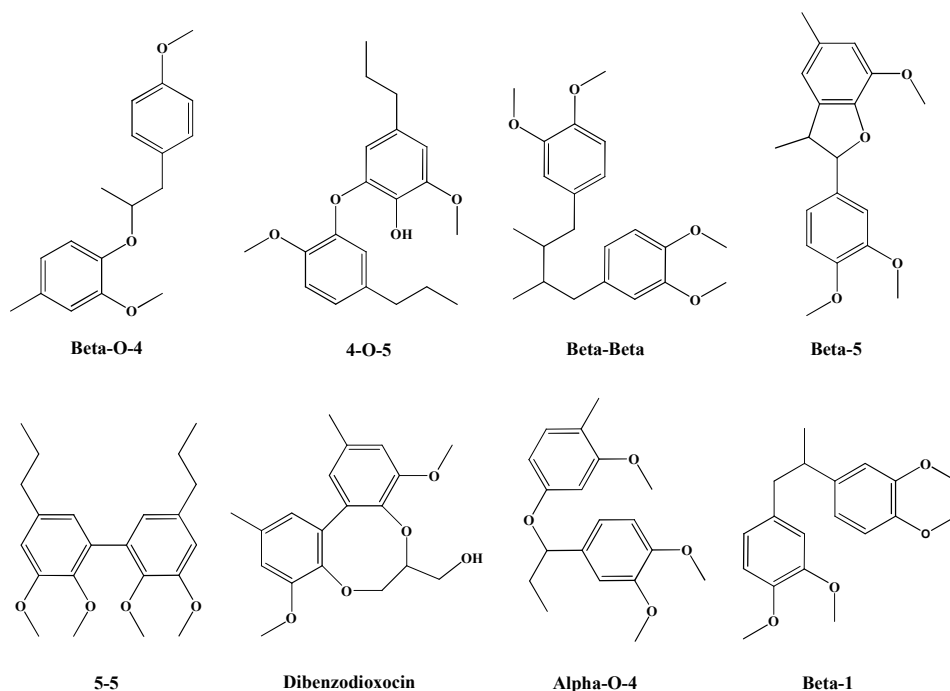
Beta-O-4 **4-O-5** **Beta-Beta** **Beta-5**

5-5 **Dibenzodioxocin** **Alpha-O-4** **Beta-1**

Figure 6 Common phenylpropane linkages in lignin. (Adapted with permission from Chakar et al., *Ind. Crop and Prod.*, 2004, **20**(2), 131-141.[121] Copyright 2004Elsevier)

Lignin has high resistance to microbial and chemical attacks due to its complex three-dimensional network formed by different non-phenolic phenylpropanoid units linked with variety of ether and C–C bonds,[62, 123] and is the most recalcitrant component of lignocellulose. Thermal pyrolysis can breakdown these phenyl-propane units of the macromolecule lattice. The pyrolysis of lignin starts with dehydration at about 200°C followed by breakdown of the β-O-4 linkage, leading to the formation of guaiacol, dimethoxyphenol, dimethoxyacetophenone (DMAP), and trimethoxyacetophenone(TMAP).[122] The β-O-4 bond scission occurs at temperatures between 250 °C and 350 °C.[124] α-, and β-aryl-alkyl-ether linkages break down between 150 and 300 °C.[62] The aliphatic side chains also start splitting off from the aromatic ring at about 300°C. Even higher temperature (370–400°C) is required to break the C-C bond between lignin structural units.[62] More generally, there are three kinds of bond cleavage including two C–O bond cleavages and one side chain C–C bond cleavage. The cleavage of a methyl C–O bond to form two-oxygen-atom products is the first reaction to occur in the thermolysis of 4-alkylguaiacol at 327–377°C. Then the cleavage of the aromatic C–O bond leads to the formation of one-oxygen-atom products. The side chain C–C bond cleavage occurs between the aromatic ring and an α–carbon atom. However, the product distribution varies with the source of biomass. Guaiacol is the main product from coniferous wood while guaiacol and pyrogallol dimethyl ether are dominant from deciduous woods.[62, 125] Lignin produces more char and tar than wood despite the higher methoxyl content of lignin.

2.1.5. Fast pyrolysis with reactive gas

Fast pyrolysis is usually performed in the absence of oxygen using nitrogen as the carrier gas. However, other carriers such as H_2, CO_2, CO, CH_4, steam, and even oxidative atmospheres have also been investigated to different extents.[126-133] Water is one of the major products of lignocellulose biomass pyrolysis. Steam was found to enhance the thermal degradation of wood

and lower the activation energy.[126] The decomposition temperature of cellulose was lowered in the presence of steam.[127] Steam also enhances the heat transfer and favors the fast desorption of low molecular weight products, which leads to higher bio-oil yield and dominant water-soluble polar products.[98, 107, 134-139] Another major effect of steam is a 30–45 wt% decrease in coke formation.[138, 140]

In the presence of hydrogen, char formation was suppressed but the gas yields and liquid product composition were not significantly affected. The product distribution and bio-oil composition were quite different when a hydroprocessing catalyst such as supported Mo-sulfide was introduced. Catalytic hydropyrolysis led to higher bio-oil yield with simpler composition and reduced oxygen content.[128, 129] In hydropyrolysis of rice husk, the presence of a catalyst led to about 16% less oxygen than that without catalyst.[130] Hydrogen pressure is a significant parameter in this process.[128] Increasing hydrogen pressure decreased both the oxygen content and the extent of overall aromatization of bio-oil.[129] Increasing the pyrolysis temperature from 500 to 650°C further decreased the oxygen content. However at low pyrolysis temperatures (375–400°C), hydrogen has only a minimal effect on product distribution and bio-oil composition, particularly at low hydrogen pressure (2 MPa).[131]

Generally CO, CO_2, CH_4, and H_2 are present in recycled pyrolysis gas. Those gases are also tested as biomass pyrolysis media.[132, 133] It was found that CO atmosphere gave the lowest liquid yield (49.6%) while CH_4 atmosphere gave the highest (58.7%).[133] More oxygen was converted into CO_2 and H_2O under CO and H_2 atmospheres, respectively. The higher heating value (HHV) of the resulting bio-oil is increased comparing to that obtained under inert atmosphere. Fewer methoxyl-containing compounds and more monofunctional phenols were found when using CO and CO_2 as carrier gases.[133] Syngas was found to be an economic alternative to pure hydrogen in hydropyrolysis of coal.[141, 142] The weight loss profiles of biomass under hydrogen and syngas were found to be almost the same. This indicates that syngas has the potential to replace hydrogen as the pyrolysis medium.[132] Mante et al. studied the influence of recycling non-condensable gases such as CO/N_2, CO_2/N_2, $CO/CO_2/N_2$, and H_2/N_2, in CFP of hybrid poplar and found it potentially increased the bio-oil yield and decreased the char/coke yield.[46]

2.2. Chemistry in catalytic fast pyrolysis

For bio-oil upgrading, many chemical routes including cracking, aromatization, ketonization/aldol condensation, and hydrotreating etc. have been extensively used to improve the quality of bio-oils.[23, 28, 143-146] CFP could integrate the fast pyrolysis and these chemical process for vapor upgrading into a simple process that could produce bio-oils with improved quality and reduced cost.[47, 48, 147] High oxygen content and the active oxygenates such as acids, ketones, and aldehydes in bio-oil are mainly responsible for the adverse attributes of bio-oils. Thus the role of a catalyst in CFP is to promote the removal of most of the oxygen in selective ways and convert the active species to stable and useful component in bio-oil. Next, we will summarize the understanding of the chemistry of the major catalytic reactions that can be used in the CFP process. It is notable that, the undergoing reactions during CFP are very complicated and the below reactions might occur simultaneously. Further efforts are still required to understand the reaction network, mechanisms, and kinetics of these reactions under the condition relevant to CFP.

2.2.1. Cracking

Aromatics and olefins can be generated from catalytic cracking of oxygenates.[148] The heavy organics that formed from re-polymerization or fragmentation can also be converted to low

molecular-weight products by cracking. Catalytic cracking chemistry of pyrolysis vapors involves conventional FCC reactions, such as protolytic cracking (cleavage of C-C bonds), hydrogen transfer, isomerization, and aromatic side-chain scission, as well as deoxygenation reactions, such as dehydration, decarboxylation, and decarbonylation.[10, 149, 150] Dehydration occurs on acid sites and leads to the formation of water and a dehydrated product. Decarboxylation and decarbonylation result in the formation of CO_2 and CO. Repeated dehydration and hydrogen transfer of polyols allows the production of olefins, paraffins, and coke.[151] Aromatics are formed by Diels-Alder and condensation reactions of olefins and dehydrated species.[151] The conceptual complete deoxygenation reaction of pyrolysis vapors predicts a maximum oil yield of 42 wt%.[10]

Hydrocarbons are formed in catalytic cracking. C_1–C_4 hydrocarbons are found to be the main cracking products over HZSM-5 from the conversion of model compounds such as acetic acid, propanoic acid, cyclopentanone, methylcyclopentanone, and alcohols like methanol, *t*-butanol, and 1-heptanol.[138, 152] Thermally stable oxygenates like sorbitol and glycerol can be converted into olefins (ethylene, propylene, and butenes), aromatics, or light paraffins (methane, ethane, and propane) while oxygen is removed as H_2O, CO, or CO_2.[151] Lignin-derived phenolics can undergo oxygen-aromatic carbon bond cleavage to form phenol/aromatic hydrocarbons or undergo oxygen-alkyl carbon bond cleavage to form benzenediols or benzenetriols. These benzenediols or benzenetriols then undergo HDO to phenol.[153] The cracking of guaiacol can be initiated by hemolytic cleavages of CH_3–O or O–H bonds and results in the production of 1,2-dihydroxybenzene, methane, *o*-cresol, 2-hydroxybenzaldehyde, and coke.[154] Thus cracking of fast pyrolysis vapors could lead to significant removal of oxygen and improvement of bio oil quality.

2.2.2. Aromatization

The abundant small-molecule oxygenates and olefins in fast pyrolysis vapor could be converted into valuable aromatics via aromatization with the oxygen rejected as CO, CO_2, and H_2O.[151, 152, 155] In the presence of HZSM-5, acids, aldehydes, esters, and furans are completely converted at temperatures above 370°C and alcohols, ethers, ketones, and phenols are also largely reduced with aromatic hydrocarbons as the main products.[152, 155, 156] High aromatic hydrocarbon yield was observed from propanal.[152] The hydrocarbon product distributions from methanol, ethanol, *t*-butanol, and 1-heptanol are strikingly similar, which suggests a common reaction pathway.[152, 157] A hydrocarbon pool mechanism is widely accepted for conversion of methanol and ethanol to hydrocarbons over HZSM-5.[157-160] Johansson et al. found significant amounts of ethyl-substituted aromatics in the hydrocarbon pool when ethanol was used as feedstock, although only methyl-substituted aromatics remained in the product.[157] Comparing the conversion of methanol, ethanol, and 2-propanol shows the high carbon number alcohol leads to quicker deactivation of aromatization activity.[8, 111, 113, 161, 162] Extensive aromatization was also found for cyclopentanone, methylcyclopentanone, acetic acid, and propanoic acid.[138] The alkylation or trans-alkylation can lead to substituted aromatic hydrocarbons. With aromatization catalyst those highly active detrimental small oxygenates in fast pyrolysis vapors could be converted into desired valuable aromatic hydrocarbons.

2.2.3. Ketonization/Aldol condensation

Pyrolysis vapors contain significant carboxylic and carbonyl components such as acetic acid and furfural. Ketonization of carboxylic acids and aldol condensation of ketones and aldehydes are able to convert those carboxylic and carbonyl components into longer-chain intermediates that can

be converted to gasoline/diesel-range products via subsequent HDO.[163-170] Esters can also undergo ketonization to form ketones.[171, 172] Ketonization forms a new ketone via C-C coupling and oxygen is rejected as CO_2 and H_2O. Acetic acid, propionic acid, hexanoic acid, and heptanoic acid were tested on a series of solid oxide catalysts at temperatures of 300–450°C.[173, 174] All these acids can be completely converted into ketones and the smaller carboxylic acid showed higher ketonization reactivity than the longer-chain acids.[173] Two aldehydes and/or ketones with at least one α-H can undergo self- or cross-aldol condensation to form a new unsaturated aldehyde or ketone with oxygen rejected as H_2O, and both Brønsted and Lewis acids are efficient catalysts for this kind of reactions.[175-181] Vapor phase condensation of propanal over a ceria-zirconia catalyst was found to proceed by both aldol condensation and ketonization pathways (**Error! Reference source not found.**).[168] Partially oxidized propanal undergoes ketonization to form 3-pentanone. 3-pentanone can react with another propanal to form 4-methyl-3-heptanone via aldol condensation. Self-aldol condensation of propanal leads to 2-methyl-2-pentenal, which forms 2-methylpentanal by hydrogenation or aromatics via further condensation (**Error! Reference source not found.**). The presence of acids inhibits the aldol condensation by competitive adsorption on active sites, and therefore a ketonization step is necessary.
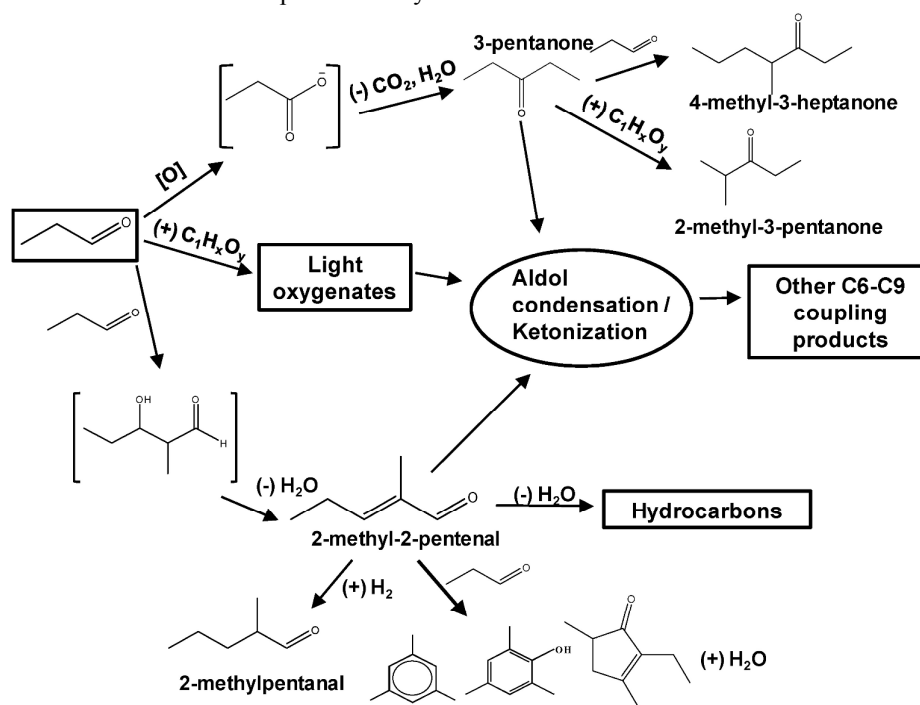
Figure 7 Proposed reaction pathway of propanal over ceria-zirconia catalyst.(Adapted with permission from Gangadharan et al., *Appl. Catal., A*, 2010, **385**, 80-91[168]. Copyright 2010 Elsevier)

2.2.4. Hydrodeoxygenation

Hydrodeoxygenation rejects the oxygen as water and retains most of the carbon in the products. A wide range of components of bio-oils can readily react with hydrogen under pressure in the presence of a proper catalyst.[182, 183] Hydrodeoxygenation of bio oil has been extensively studied and well documented during the past decades.[35, 36, 182-187] Only those conducted under atmospheric pressure have the potential to be integrated in biomass fast pyrolysis unit. Phenol and its derivatives are the least active compounds in hydrodeoxygenation but the most studied substrates in vapor phase hydrodeoxygenation over supported noble metals.[188-193]

Hydrodeoxygenation and transalkylation are the two competitive reactions of phenol derivatives. The dominant pathway depends on the catalyst composition, the properties of both the metal, and its support.[194] For instance, with low acidity support, guaiacol first undergoes demethylation to form catechol.[188, 193] Catechol is very active and undergoes sequential HDO to benzene via phenol.[188] Anisole follows a similar pathway which first demethylated to phenol.[188] With acidic support, both transalkylation and hydrodeoxygenation were achieved at significant extent.[190, 192] For carbonyl compounds such as propionic acid, 2-methylpentanal, furfuryl, decarbonylation is dominant over noble metals and hydrogenation to corresponding aldehyde and alcohol is dominant with base metal catalyst.[195, 196] Vapor phase hydrodeoxygenation is very attractive for converting those lignin derived small oxygenates.

2.2.5. Steam reforming

Pyrolysis vapor components, especially the small oxygenates, can also undergo steam reforming to produce renewable H_2.[197-203] The general reaction scheme for the steam reforming of oxygenates proceeds as Eq. (0).[200] When combined with a water-gas shift reaction the overall reaction will be Eq. (0).[200] Acetic acid and hydroxyacetaldehyde undergo rapid thermal decomposition and achieve complete steam reforming over commercial Ni-based catalysts.[199] The decomposition of acetic acid leads to formation coke, which is removed by subsequent steam reforming.[197] Hydroxyacetaldehyde is found completely decomposed on the metal catalyst surface without detectable intermediates.[197] Acetone can be completely reformed to hydrogen over Co supported on graphitized active carbon.[204] However, acetic acid undergoes rapid coking at temperatures below 650°C.[202] Besides acetic acid, m-cresol and dibenzyl ether also completely converted to hydrogen and carbon oxides above 650°C.[202] An overall positive effect on hydrogen production was observed for high concentrations of lower molecular-weight oxygenates, such as acetic acid and acetol in steam reforming of water-soluble components at 500°C.[205] The presence of steam in CFP reactor could generate a hydrogen atmosphere in the reactor by eliminating the detrimental small oxygenates via steam reforming.

$$C_nH_mO_p + (n-p)H_2O \rightarrow nCO + (n-p+m/2)H_2 \tag{0}$$

$$C_nH_mO_p + (2n-p)H_2O \rightarrow nCO_2 + (2n-p+m/2)H_2 \tag{0}$$
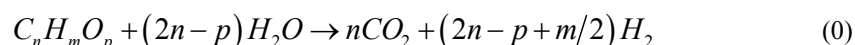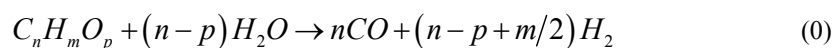
3. Catalysts for CFP of lignocellulosic biomass

Catalytic fast pyrolysis combines the fast pyrolysis of lignocellulose with the catalytic transforming of the primary pyrolysis vapors to more desirable and less oxygenated liquid fuels. Removing oxygen as CO_2 is most desirable since it would minimize the need for external H_2 and improve the H/C ratio in the final products.[56] Catalytic cracking at 300–500°C can produce liquid hydrocarbons from oxygenates, with the oxygen removed in the form of H_2O, CO, and CO_2 and coke. Catalytic cracking is generally performed at atmospheric pressure and without a hydrogen requirement. Solid acids such as zeolites, silica-alumina, silicalite, FCC catalysts, alumina, molecular sieves, as well as metal oxides such as zinc oxide, zirconia, ceria, and copper chromite have been studied as catalysts in catalytic cracking of pyrolysis vapors.[155, 206-210] Besides those solid catalysts, other inorganic materials including metal chlorides, phosphates, sulfates, and alkali have also been investigated in CFP of biomass.[43, 56, 95, 211-213] They can be categorized into several groups including soluble inorganics, metal oxides, microporous materials, mesoporous materials, and supported metal catalysts.

As mentioned in Section 1, catalysts can be mixed either directly with biomass feedstock in the fast pyrolysis reactor or only with the hot pyrolysis vapor after the fast pyrolysis reactor, *i.e.*, *in situ* and *ex situ* CFP.[40] The processes may have different advantages and disadvantages although the catalysts play a similar role in each. The effects of various catalysts on both *in situ* and *ex situ* CFP of lignocellulosic biomass in terms of bio-oil yields and selectivity to desirable products will be included in the current discussion.

3.1. Soluble inorganics

Biomass contains certain amounts of inorganic species such as K, Na, Ca, and P (see Table 3).[214-216] The presence of inorganic materials influences the thermal properties of each component of lignocellulose.[217, 218] It is well known that small amounts of mineral matter naturally present in whole biomass samples strongly catalyze the decomposition of the cellulose component.[65] Generally the presence of inorganics increases the yield to solid products and decreases the yield to gaseous products.[211, 215, 216, 219] These inorganics, especially K and Ca, catalyze the decomposition of biomass and promote char formation.[214, 215, 220, 221] Potassium was found to catalyze pyrolytic reactions and promote the formation of CO_2 and CO from polysaccharides, acetic acid from hemicellulose, formic acid from polysaccharides, and methanol from lignin.[215, 222]

Soluble inorganics affect the pyrolysis temperature, product distribution, and yields of biomass. A systematic examination of the effect of KCl on the pyrolysis of wheat straw and single biopolymers (cellulose, xylan, and lignin) showed that the presence of 2 wt% KCl significantly increased the char yield and decreased tar yield. The yields to char, tar, and gases from cellulose were highly influenced by the presence of KCl, whereas xylan and lignin were influenced to a less extent.[215] $MgCl_2$, NaCl, $FeSO_4$, and $ZnCl_2$ also increased the char yield in sugar cane bagasse pyrolysis.[223] Using TGA with mass spectroscopy, Varhegyi et al. found that impregnating 1 mol% each of $MgCl_2$, NaCl, $FeSO_4$, and $ZnCl_2$ on the microcrystalline cellulose dramatically changed in the product distribution, characteristic decomposition temperature, and weight loss.[95, 223] $MgCl_2$ doesn't affect weight loss or decomposition temperature of cellulose but suppresses the yield to aldehydes, ketones, furans, and 2-furfuraldehydes. NaCl leads to lower onset temperature and higher ending temperature in cellulose decomposition and increases the total amount of low molecular-weight products by a factor of about three. In addition, due to the strong inhibition of transglycolylation reactions by sodium, the presence of NaCl dramatically suppresses formation of levoglucosan (0.4 wt%) compared to that of the pyrolysis of untreated cellulose (36 wt%).[95, 224, 225] $FeSO_4$ catalyzed both the formation of levoglucosan and levoglucosenone from wood and decreased the decomposition temperature of cellulose by 50°C.[95, 223, 226] Chlorides including $CuCl_2$ and $FeCl_2$ also promoted the yield to levoglucosan.[226] $ZnCl_2$ led to two decomposition peaks of cellulose with the lower one associated with dehydration reactions and the higher one resembling that of the untreated sample. Pyrolysis of corncob impregnated with 15 wt% $ZnCl_2$ in a lab-scale downflow reactor at about 340°C yielded more than 8 wt% furfural and 4 wt% acetic acid, which account for over 50 wt% and 25 wt% of pyrolytic liquids on a water-free basis, respectively.[227] More recently the alkali and alkaline earth metal chlorides were found to affect cellulose pyrolysis in different ways although both of them significantly changed the low molecular-weight product composition.[228] Alkaline earth metal chlorides ($MgCl_2$ and $CaCl_2$) substantially reduced the weight loss temperature of cellulose while alkali metal chlorides (NaCl and KCl) did not change that temperature much. Those cholorides indicate that the cations are critical for the catalytic activity.

Table 3 Composition of switchgrass ash. (Adapted with permission from Patwardhan et al.,

Bioresour. Technol., 2010, **101**, 4646-4655.[229] Copyright 2010 Elsiever)

Compound	Content (wt%)
SiO_2	72.2
Al_2O_3	3.74
Fe_2O_3	1.28
SO_3	0.39
CaO	6.19
MgO	2.33
Na_2O	0.77
K_2O	6.17
P_2O_5	2.63
TiO_2	0.18
SrO	0.02
BaO	0.01
Loss on ignition @750°C	1.63

In fact, both cations and their anion counterparts affect the yield to levoglucosan from cellulose pyrolysis.[229] The reduction of levoglucosan yield follows the trends of $K^+ > Na^+ > Ca^{2+} > Mg^{2+}$ for cations and $Cl^- > NO_3^- \approx OH > CO_3^{2-} \approx PO_4^{3-}$ for anions.[229] Alkaline sodium compounds NaOH, Na_2CO_3, and Na_2SiO_3, promoted the yield to acetol and favored H_2 formation in microwave pyrolysis of pine wood.[211] Phosphorus (H_3PO_4 and $(NH_4)_3PO_4$) promoted the yield to furfural and levoglucosenone from cellulose via new rearrangement and dehydration routes.[216] The presence of inorganics could also catalyze the carbonization reactions of the lignin moiety in lignocellulose and lead to higher char yield.[230] The effect of impregnation of 2 wt% each of $Na_2B_4O_7 \cdot 10H_2O$, NaCl, $KHCO_3$, $AlCl_3 \cdot 6H_2O$, and $NH_4H_2PO_4$ on the pyrolysis of wood, α-cellulose, and lignin was investigated by dynamic TGA.[231, 232] The presence of those inorganics led to a decrease in the pyrolysis temperatures of wood and α-cellulose,[231, 232] likely due to the acid-base property of those inorganic species that catalyze the depolymerization/decomposition of cellulose.[65] However such decreasing pyrolysis temperature is less pronounced for lignin.[231, 232]

3.2. Metal oxides

Metal oxides, particularly transition metal oxides, have been widely used as heterogeneous catalysts in various reactions.[233, 234] Generally, metal oxides possess either redox properties due to their multivalent nature and/or certain acid-base properties which could potentially catalyze the thermal decomposition of lignocellulose and/or the reaction of pyrolysis intermediates to form more stable products.[233-235] Various metal oxides, including MgO, NiO, Al_2O_3, ZrO_2, TiO_2, MnO_2, CeO_2, Fe_2O_3, and their mixtures, have been tested as catalysts for CFP.

3.2.1. Acidic metal oxides

Acidic metal oxides such as Al_2O_3, SiO_2, and SiO_2-Al_2O_3 as well as the sulfated metal oxides such as SO_4^{2-}/TiO_2, SO_4^{2-}/ZrO_2, and SO_4^{2-}/SnO_2 have been investigated as catalysts in CFP.[212, 236-239] Addition of acidic metal oxides led to the decrease of liquid yield and increase of gas and solid yields.[212] For instance, the presence of Al_2O_3 decreased the liquid yield from 58.6 wt% to about 40 wt% in *ex situ* CFP of Lignocel HBS 150-500 with a fixed-bed reactor.[212] In particular, the yield to organics decreased from 37.37 wt% to about 7 wt%, while the yield to water increased from 21.38 wt% to about 32 wt%, compared to non-catalytic pyrolysis.[212]

The presence of acidic metal oxides also changes the composition of bio oil. For

17

Al_2O_3-catalyzed pyrolysis, there were much more aromatic hydrocarbons and polycyclic aromatic hydrocarbons (PAH) in the organic products. SiO_2 of weak acidity and medium porosity was active in removing oxygenated compounds such as acids, ketones, and aldehydes and in inhibiting coke and polycyclic aromatic compound formation in CFP of *Jatropha* residue.[237] Acidic metal oxides also catalyze the decarbonylation reactions and lead to the increase of CO.[212] Meanwhile the yields to C_1–C_4 hydrocarbons are also greatly increased.[212]

The different nature of the acidity acts different. The strong Brønsted acids, such as SO_4^{2-}/TiO_2, SO_4^{2-}/ZrO_2, and SO_4^{2-}/SnO_2 significantly decreased the yields to levoglucosan and hydroxyacetaldehyde, and greatly increased the yields to 5-methylfurfural, furfural, furan, and levoglucosenone in cellulose pyrolysis.[238, 239] SO_4^{2-}/SnO_2 was most selective to 5-methyl furfural, while SO_4^{2-}/TiO_2 and SO_4^{2-}/ZrO_2 were more favorable to furfural and furan respectively.[238] On the other hand, Fabbri et al. found that the Lewis acid, Al_2O_3 nanopowder, led to higher overall yields to anhydrosugars from cellulose.[236]

3.2.2. Basic metal oxides

Base oxides are known active catalysts for ketonization and aldol condensation of carboxylic acid and carbonyl compounds. Alkaline earth metal oxides such as MgO and CaO are classic base catalysts, where oxide ions behave as bases and the metal cations can function as Lewis acids.[233] The addition of MgO decreased the yield to bio-oil but improved the bio-oil quality in terms of heating value, hydrocarbon distribution, and removal of oxygenated groups.[212, 240] The oxygen content of bio-oil decreased from 9.56 wt% to 4.9 wt% in the presence of MgO.[240] And with MgO, the carbon backbone of aliphatic hydrocarbons in bio-oil decreased from C_{22}—C_{28} to C_{11}—C_{17}.[240] In contrast to the effect of acidic oxides, the presence of MgO significantly increased the yield to CO_2 by catalyzing the ketonization of carboxylic acids.[212] Lu et al. found that the activity of nano MgO to alter the pyrolytic products was between those of ZnO and Fe_2O_3.[213] Lu et al.found nano CaO reduces the selectivity to phenols and anhydrosugars from 26.5% and 10.1% to 13.0% and 1.2%, respectively, in non-catalytic fast pyrolysis. CaO eliminated the acids and increased the ketone selectivity from 3.8% to 20.9%, particularly the selectivity to cyclopentenones, which increased to 16.7% from 2.4%.[213] Meanwhile the levels of hydrocarbons and light compounds (acetaldehyde, acetone, 2-butanone, and methanol) were also greatly increased compared to non-catalytic pyrolysis.[213] Basic metal oxides are able to improve the quality of bio oil.

3.2.3. Other transition metal oxides

Besides classic basic and acidic metal oxides, transition metal oxides such as NiO, tetragonal ZrO_2, ZnO, TiO_2, Fe_2O_3, CeO_2, MnO_2, and binary transition metal oxides such as ZrO_2/TiO_2, Mn_2O_3-CeO_2, and ZrO_2-CeO_2 have also been investigated in CFP of biomass.[163, 174, 212, 213, 241, 242] TiO_2, Fe_2O_3, NiO, and ZnO catalysts can decrease the liquid and organic product yields and increase the gas, water, and solid products yields.[213] Particularly CO_2 yield increased in the presence of NiO and ZrO_2/TiO_2. And the simultaneous increase of CO_2 and H_2 in gas products indicates the increase of CO_2 yield over NiO is more likely due to the steam reforming.[212] Formation of various hydrocarbons was found over Fe_2O_3 and ZrO_2/TiO_2 but the yield is poor.[212, 213] Catalytic fast pyrolysis of rice husk with ZnO decreased the bio-oil yield but enhanced the yields to small molecular compounds and decreased the amount of oxygenated groups in bio-oils.[241] ZnO also promotes hydrogen atom transfer in the cracking process.[243] FeO-Cr_2O_3 oxides were found lead to selective production of phenol and light phenolics at 500°C.[206]

SiO_2-supported CeO_2, Fe_2O_3, ZnO, MnO_2, and MgO, as well as mixed metal oxides such as

Mn_2O_3-CeO_2 and ZrO_2-CeO_2 were investigated for the potential of catalyzing ketonization and aldol condensation of carbonyl compounds in pyrolysis vapor.[163, 174, 242] In this case, smaller carboxylic acid molecules like acetic acid and propanoic acid could be converted to gasoline-range organics, while the oxygen of carboxylic acid is rejected as CO_2 and water. CeO_2 is highly active for this purpose and tolerant to water. Employing Al_2O_3 and TiO_2 as supports or doping with a strong base can improve the catalytic activity. Water and phenols have only minor influence on ketonization of acetic acid. Furfural strongly inhibits the ketonization. Ceria-based mixed metal oxides like Mn_2O_3-CeO_2 and ZrO_2-CeO_2 are more active than CeO_2 itself.[163] Mn_2O_3-CeO_2 has the highest tolerance to both CO_2 and water.[163] Mixed zinc and zirconium oxide are also capable of converting small oxygenates into larger hydrocarbons at moderate temperature and atmosphere pressure.[158, 244, 245] In addition to the facile reduction/oxidation, acid-base properties of the transition metal oxides also seem related to their performances.

3.3. Microporous materials

Microporous materials have been successfully employed in FCC in petroleum refineries and methanol-to-gasoline processes. Taarning et al. reviewed the applications of zeolites in biomass conversion to fuels and chemicals.[41] In particular, the potential of using microporous materials to catalyze the fast pyrolysis of lignocellulosic biomass has been extensively studied in the past two decades due to their well-known acidic properties and shape selectivity. Investigation of a larger variety of zeolites with various pore sizes and shapes in CFP of glucose and biomass indicated that zeolites of medium pore size, moderate internal pore space and steric hindrance are the most promising catalysts for aromatic production.[246, 247]

3.3.1. ZSM-5

A large variety of microporous materials have been studied for their application in CFP of lignocellulosic biomass. ZSM-5 based catalysts have been most extensively studied, especially the protonated one, HZSM-5, due to its strong acidity and shape selectivity. As a shape-selective zeolite, HZSM-5 has intermediate pore sizes (0.54×0.56 nm), and good thermal and hydrothermal stability.[248] Only small molecules are allowed to diffuse into the micropores and be restructured to large molecules with folded effective sizes not larger than trimethylbenzene.[138] HZSM-5 is the most effective catalyst for aromatic hydrocarbon production from the pyrolytic vapors.[155, 246, 249, 250]

HZSM-5 is most selective to produce aromatic hydrocarbons from bio-oil vapors.[138] Adjaye et al. compared the activity of HZSM-5, silicalite, H-mordenite, HY, and silica-alumina in catalytic cracking of maple wood bio-oil vapors with a fixed-bed microreactor at 290–410°C, and found that strong-acid shape-selective HZSM-5 zeolites led to the most aromatics.[155] A similar conclusion was reached while comparing the activity of clinoptilolite, HZSM-5, and HY in *ex situ* CFP of olive residue with a two-stage fixed-bed reactor.[208] The resulting oil obtained over HZSM-5 may be readily separated from the aqueous phase.[251] Both lignin derivatives and products from biomass pyrolysis were selectively converted into aromatic hydrocarbons over HZSM-5 at 350–410°C.[252, 253] Cracking, deoxygenation, decarboxylation, cyclization, aromatization, isomerization, alkylation, disproportionation, oligomerization, and polymerization were the main reactions in the catalytic cracking process.[138, 252, 254-256] Introducing steam into the system enhanced the yield to organic distillate and slightly decreased the aromatic hydrocarbon selectivity.[138]

The presence of ZSM-5 markedly reduced the yield to oil, and oxygen was found mainly

rejected as H_2O at lower reaction temperature and as CO_x at higher temperatures.[257] Single-ring aromatics as well as PAH were the main components of the resulting bio-oil.[257] Williams et al. suggested a dual mechanism for the formation of aromatics and PAH in the zeolite cracking process: (1) formation of short-chain hydrocarbons on the catalyst, which then undergo aromatization to form aromatics and PAH; (2) deoxygenation of oxygenates found in the non-phenolic fraction of the pyrolysis oils, which directly form aromatics.[258] Zhang et al. compared the non-catalytic fast pyrolysis and the *in situ* CFP of corncob on HZSM-5 in a fluidized-bed reactor at 400–700°C. It was found that the presence of HZSM-5 increased the yields to non-condensable gas, water, and coke while decreased the liquid and char yields.[259] The CFP with ZSM-5 leads to a decrease of more than 25% in the oxygen content of the resulting bio-oil.[259]

3.3.1.1. Deoxygenation mechanism on ZSM-5

In CFP, lignocellulose is first thermally decomposed into the corresponding monomers of each component and to smaller oxygenates. These fragments then contact the catalyst and undergo further transformation. The shape-selective and strongly acidic HZSM-5 can catalyze a wide range of reactions. Different oxygenates lose their oxygen and convert to aromatic hydrocarbons over HZSM-5 under different conditions and in different ways (Table 4).[41, 260, 261]

Table 4 Formation of H_2O, CO, and CO_2 for various oxygenates over HZSM-5.(Adapted with permission from Taarning et al., *Energ. Environ. Sci.*, 2011, **4**, 793-804.[41] Copyright 2011 Royal Society of Chemistry)

Feed compound	Oxygen in gas phase (%)		
	H_2O	CO	CO_2
Methanol	100	0	0
Dimethyl ether	100	0	0
Guaiacol	96	3	1
Glycerol	92	7.5	0.5
Xylenol	93	6	1
Eugenol	89	9	2
Anisole	88	12	Trace
2,4-dimethyl phenol	87	12	1
o-cresol	80	17	3
Starch	78	20	2
Isoeugenol	77	19	4
Glucose	75	20	5
Dimethoxylmethane	73	6	21
Xylose	60	35	5
Sucrose	56	36	8
n-butyl formate	54	46	0
Diphenyl ether	46	46	8
Furfural	14-22	75-84	2.5-3.0
Methyl acetate	54	10	36
Acetic acid	50	4	46

Different type of oxygenates react differently on ZSM-5 and the reaction temperature affects the product distribution. Gayubo et al. found that alcohols (methanol, ethanol, 1-propanol,

2-propanol, 1-butanol, and 2-butanol) undergo dehydration over HZSM-5 at low temperatures (above about 200°C) to form olefins, which are converted to higher olefins above 250°C and then to alkanes and aromatics at higher temperatures (above 350°C).[260-262] Aldehydes like acetaldehyde are very active and form large amounts of thermal coke instead of hydrocarbons over HZSM-5.[261] Such thermal degradation of aldehydes, phenols, and pyrolytic lignin could lead to reactor plugging.[262] Hoang et al. compared the conversion of propanal and propylene on HZSM-5 and found that propanal is more active than propylene.[263] Propanal was converted to C_9 aromatics via formation of an aldol trimer followed by dehydration and cyclization, which is different from the well-known carbon-pool mechanism of propylene. Carboxylic acid and ester functionalities favored oxygen removal through decarbonylation over dehydration, which preserved hydrogen in the hydrocarbon products.[264] According to the conversion data of ketones and acetic acid over HZSM-5 reported by Gayubo et al.,[261] ketones underwent condensation and decomposition to form aromatics and olefins, as evidenced by the consumption of ketones accompanied by simultaneous evolution of H_2O. Acetic acid first underwent ketonization to form acetone, as evidenced by the simultaneous evolution of acetone, CO_2, and H_2O.[261] Then it followed the same reaction pathways of acetone to form aromatics and olefins. The conversion of glucose on HZSM-5 proceeded in two steps. Glucose first thermally decomposed to smaller oxygenates through retro-aldol fragmentation, dehydration, and Grob fragmentation, which generates two aldehydes, such as glucose, from 1,2,3-triol.[108, 156] In the second step, the dehydrated intermediates converted into aromatics, CO, CO_2, and water over the catalyst. The catalytic conversion step is significantly slower than the initial pyrolysis reaction of glucose.[156] The first step of furfural conversion is the decarbonylation to furan; furan converts to intermediates like cyclohexene and 3,4-dimethylbenzaldehyde, and then to aromatics, light olefins, carbo oxides, and coke.[243] Zhao et al. studied catalytic cracking of 5-hydromethylfurfural over HZSM-5, Ga/HZSM-5, In/HZSM-5, and β-zeolite and found that HZSM-5 is the most active catalyst.[265]

Phenol is much less reactive than other substrates and is only partially converted to propene and butenes at 400°C.[260] Guaiacol is more difficult to convert on HZSM-5 even at 450°C. Guaiacol increased the coke deposition on the cracking catalysts.[260, 266] In CFP of lignin, the depolymerized lignin products underwent consecutive reactions to form alkoxy phenols, phenols, and eventually aromatic hydrocarbons.[267] Mullen and Boateng studied the catalytic pyrolysis of lignin over HZSM-5 and found HZSM-5 deepened the depolymerization of lignin.[268] The aliphatic linkers of the lignin aromatic units were converted into small olefins, which can undergo aromatization to hydrocarbons.[268] The partial deoxygenation of lignin aromatic units produces simple phenols.[268] Zhao et al. achieved a selectivity to aromatic hydrocarbons above 87% by *in situ* CFP of pyrolytic lignin over non-protonized ZSM-5 at 600°C with a fixed-bed reactor.[82] HZSM-5 led to about 50% more coke deposition than its non-protonized counterpart due to its stronger acidity.[82] Bulkier monolignols derived from syringyl lignin were not effectively converted by HZSM-5 due to size exclusion or pore blockage.[269]

3.3.1.2. Role of acidity

Acidity, particularly Brønsted acidity, is critical for cracking the oxygenates in pyrolysis vapor.[247, 270] The acidic sites of HZSM-5 promote deoxygenation, decarboxylation, and decarbonylation of oxygenate components, as well as cracking, oligomerization, alkylation, isomerization, cyclization, and aromatization via a carbonium ion mechanism.[270, 271] Substitution for H with K led to almost complete loss of its activity.[250] Even partly neutralizing HZSM-5 by 1.5

wt% potassium doping led to a drastic decrease in the selectivity to gasoline.[272] The strong-acid shape-selective HZSM-5 zeolites produce mostly aromatics, while HY zeolites and silica-alumina produce mainly aliphatic hydrocarbons.[155, 208] Theoretically, higher acidity of a catalyst should increase the activity of cracking.[249] The better hydrogen transfer capability of HZSM-5 is mainly responsible for its producing the highest yield to hydrocarbons.[41, 155, 272] The acidity of HZSM-5 can be tuned by varying the Si/Al ratio of the framework (**Error! Reference source not found.**). Generally the low Si/Al ratio implies a relatively high acidity. Li et al. found that both decreasing the Si/Al ratio and increasing the catalyst-to-feed ratio increases the yield to aromatic hydrocarbons.[273] Mihalcik et al. demonstrated similar effects of Si/Al ratio on the deoxygenation of the pyrolysis vapors toward aromatic hydrocarbons.[249] Foster et al. found that the concentration of acid sites inside the zeolite is critical for maximizing aromatic yield.[274] The aromatic yield from glucose conversion goes through a maximum as a function of the Si/Al ratio of the ZSM-5 framework.[274] However, a low Si/Al ratio can also lead to relative instability of the catalyst framework due to dealuminization under hydrothermal conditions. Thus ability to fine tune the acidity without sacrificing the stability of catalysts is desirable.

3.3.1.3. Effect of reaction conditions

Reaction temperature, residence time, promoter, and catalyst-to-feed ratio are all important factors affecting product distribution and coke formation in the cracking process.[156, 243, 257, 275, 276] The fast heating rates, high catalyst-to-feed ratio, and proper catalyst selection are crucial to maximize the desired product yield.[49, 207] Horne et al. diluted the catalyst bed with steel ball bearings and observed increased yields to aromatics and PAH due to the decrease of the gas hourly space velocity.[277] From the *in situ* CFP of wood sawdust with HZSM-5 in a fluidized-bed reactor, Carlson et al. found that the yield and selectivity can be controlled by weight hourly space velocity (WHSV) and reaction temperature.[278] Lowering biomass WHSV and reaction temperature both lead to higher yields to monocyclic aromatics.[278] Lowering biomass WHSV also decreases the selectivity to polycyclic aromatics.[278] Increasing residence time also led to rejection of more oxygen as CO_2 and CO.[279] Increasing the catalyst-to-bio-oil feed ratio also increases the yields to gasoline and middle distillates and decreases coke formation.[49, 207, 275]

Co-feeding of small alcohols such as methanol, 1-propanol, 1-butanol, and 2-butanol with pine wood increases the effective H/C ratio and leads to higher aromatic hydrocarbon yield and longer catalyst lifetime.[264, 280] Co-processing of pyrolysis vapors and methanol showed that the presence of methanol led to more oxygen in pyrolysis vapor rejected as water and less as carbon oxides.[281, 282] The formation of hydrocarbons seems to compete with decarbonylation and decarboxylation.[282] Co-feeding of methanol with pyrolysis vapor produced less CO and CO_2 from pyrolysis vapor and improved the hydrocarbon formation.[282] The co-processing also resulted in a large increase in alkylated phenolics and aromatic hydrocarbons, and decrease in undesired heavy 3-, 4-, and 5-ring PAH.[281] Co-pyrolysis of cellulose and low density polyethylene—a surrogate for waste plastics as an effective hydrogen source—led to higher aromatic carbon yields, higher selectivity to monoaromatics and less coke formation from cellulose.[283] The effective hydrogen of the feed is a known critical factor to CFP performance.[264, 284] The hydrogen-rich co-feeding is expected to enhance performance.[41, 285] The sweeping gas also affects the yield of products in CFP, and steam improves the quality and yield to liquid products.[140] Application of hydrogen as carrier gas led to significant change of product distribution in CFP of biomass.[286] A significant decrease in acetic acid was observed over both HZSM-5 and Ni/ZSM-5 catalysts.[286] Although the increase

of hydrogen pressure from 100 psi to 400 psi did not increase the aromatic hydrocarbon yield, it led to an increase in the selectivity to benzene and toluene accompanied by a decrease of xylene.[287]

3.3.1.4. Deactivation

The activity of HZSM-5 decreases with increasing regeneration, as evidenced by increasing oxygen content, increasing molecular weight range of the upgraded oil and decreasing concentration of aromatic hydrocarbons and PAH.[258] Coke deposition leads to blockage of both active sites and micropores, which is one of the major causes of catalyst deactivation.[288] Aldehydes, phenols, and pyrolytic lignin are the most suspected coking precursors.[262] Coke formation is more severe at higher reaction temperatures.[252, 289] Deactivation by coke deposition in transformation of the aqueous fraction of bio-oil is similar to that in transformation of light oxygenates such as in methanol and ethanol conversion.[262] Guaiacol was also responsible for an increase of coke deposition when co-processed with n-heptane and gasoil.[266] However, coke deposition does not change the strength of the acidic sites on HZSM-5; it only decreases the total number of acid sites as they are covered by coke.[260, 290] Both Brønsted and Lewis acid sites are affected by coke deposition, and it is more severe on Brønsted sites.[290] The deactivation rate by coke deposition from alcohols is slower than from other oxygenates such as aldehyde, ketones, and carboxylic acids.[261, 262] The presence of water inhibits coke formation due to partial reforming by steam.[138, 254, 282] The effective hydrogen of the feed is also critical to minimize coke formation and maximize hydrocarbon production.[284]

Co-feeding with low effective H/C ratios leads to more pronounced deactivation.[264] Methanol attenuates coke formation.[280] Dilution with methanol improves the lifetime significantly.[264] Thus, hydrogen-rich co-feeding is very helpful.[41, 285] Generally, deactivation by coke deposition is reversible. The catalyst can be regenerated by coke combustion.[262]

Another cause of deactivation is dealumination due to high water content and high reaction temperature.[262, 290] Deactivation by dealumination is evident at 450°C with high-water-content feed.[290] Deactivation by dealumination is irreversible due to the disappearance of a significant number of acidic sites, particularly the stronger ones. Dealumination leads to drastic deterioration of total acidity of the catalyst. As with the deactivation of coke formation, both Brønsted and Lewis acid sites are affected by dealumination. Brønsted sites are more affected under moderate dealumination conditions and Lewis sites are more affected under severe dealumination conditions. The localized hot spot in catalyst regeneration is also responsible for the irreversible deactivation of catalysts.[270] Temperatures below 400°C are recommended to avoid irreversible deactivation of the catalyst.[261] Metal impurities deposit on the catalyst after several reaction-regeneration cycles, but the acid sites on the zeolites are not affected.[278]

3.3.1.5. Metal-modified ZSM-5

The composition of the desired liquid hydrocarbon products could be tuned by choosing the proper type of catalyst.[155] It is known that acidity and porosity of the zeolite is critical for aromatic yields.[250] Besides varying the Si/Al ratio, doping of other metal cations or oxides into zeolites such as ZSM-5 is another efficient way to finely tune the strength and density of the active sites. Various metal-modified ZSM-5 catalysts were tested in CFP of biomass and CeZSM-5, CoZSM-5, H/[Al,Fe]ZSM-5, GaZSM-5, H/[Co]ZSM-5, NiZSM-5, and HZSM-5 were found to be the most promising catalysts for hydrocarbon production.[291]

Bifunctional property was introduced to HZSM-5 by metal mofification. Park et al. compared

HZSM-5 and Ga-modified HZSM-5 in *ex situ* CFP of pine sawdust at 400°C.[292] Ga/HZSM-5 showed higher bio-oil yield and also higher selectivity to aromatics. In particular, yields to both aromatics and benzene, toluene, and xylenes (BTX) over Ga/HZSM-5 are about twice that over HZSM-5 catalyst. Cheng et al. further demonstrated that addition of Ga to ZSM-5 can increase the production rate of aromatics in CFP.[50] Ga/HZSM-5 appears to be a bifunctional catalyst, where Ga species increase the rate of decarbonylation and olefin aromatization while ZSM-5 catalyzes other reactions such as oligomerization and cracking for the production of aromatics.[50] Further modifying of the pore openings of Ga/ZSM-5 by silylation led to very high selectivity to *para*-xylene due to more space confinement.[293]

Zn showed promoting effect of on HZSM-5 in CFP of furfural.[243] Zinc promoted hydrogen atom transfer during the process.[243] Doping of zinc improved the conversion of the decarbonylation product (furan) and yielded more benzene, carbon oxides, and alkene than the parent HZSM-5.[243] As shown in Table 5, the total acid amount was barely affected by the doping of Zn even when Zn loading increased from 0.5% to 1.5%.[243] However, it did change the nature and the distribution of the acid sites. Some of the Brønsted acid sites were converted into Lewis acid sites, and the extent increased with increased zinc loading. Alkylation of benzene was retarded by increasing zinc content on Zn/HZSM-5.[243] Increased zinc loading also led to less graphite-like coke deposition compared to HZSM-5. [243] For 1.5% Zn/HZSM-5, oxygenated coke became dominant on the catalyst surface. Those promoting effects are possibly due to the capability of Zn to activate C-H bonds. The activated hydrogen atoms are then transferred to adsorbed carbenium by Brønsted acid sites in the vicinity.

Table 5 Characterization of acid sites of HZSM-5 and Zn/ZSM-5.(Adapted with permission from Fanchiang et al., *Appl. Catal., A,* 2012, **419–420**, 102-110.[243] Copyright 2012 Elsevier)

Sample	Acid site type	Peak position, °C	FWHM, °C	Acid site content, %	Total sites, mmol/g
HZSM-5	Lewis	177	47	16.2	0.36
	Brønsted	365	132	84.8	
0.5% Zn/HZSM-5	Lewis	198	88	29.4	0.37
	Brønsted	343	140	70.6	
1.5% Zn/HZSM-5	Lewis	216	98	47.	0.39
	Brønsted	338	136	52.8	

FWHM: Full width at half maximum

Ni and Co introduce steam reforming active sties to HZSM-5. Doping various amounts of Co and Ni onto ZSM-5 also decreased Brønsted acid sites and increased Lewis acid sites**Error! Reference source not found.**.[294] However the total quantity of acid sites seems quite constant even when metal loading increases from 1% to 10%.[294] Incorporation of transition metals (Ni or Co) in a commercially diluted ZSM-5 catalyst induced relatively small but noticeable changes in the performance of original ZSM-5. The metal-modified ZSM-5 showed limited reactivity toward water production.[294] A significant increase of H_2 in gas products was observed on Ni- and Co-doped ZSM-5, which seems to be due to steam reforming over metallic Ni and Co. The reduction of metal phases during pyrolysis was verified by detailed x-ray diffraction and high

resolution transmission electron microscopy analysis. [294] The presence of metallic Ni and Co can favor hydrogen transfer reactions and enhance hydrogenation.[294]

Incorporation of Fe and Cu to HZSM-5 does not significantly alter the product yields. Companella and Harold compared the activities of HZSM-5, Fe-ZSM-5, Cu-ZSM-5, and Ni-ZSM-5 in CFP of microalgae.[140] Doping with Fe, Cu, and Ni slightly decreased the liquid yield and increased the gas yield, while the char yield remained almost the same as on HZSM-5.[140] However, according to the specific analysis results of the liquid products they reported, the deoxygenation extent on those metal-doped ZSM-5 catalysts was lower than that on HZSM-5.[140] The decrease of liquid yield and deoxygenation extent could be due to the acidity change on those catalysts, while the increase in gas products could be associated with the reforming of certain intermediates on these metal sites. Melligan et al. found that doping with Ni led to lower amounts of the higher molecular-weight phenolic compounds and larger amounts of lighter phenols in CFP of *Miscanthus x giganteus* with a Py-GC/MS system.[286]

Thangalazhy-Gopakumar et al. modified ZSM-5 with Ni, Co, Mo, and Pt, which showed higher aromatic yield than their HZSM-5 counterpart (~42.5 wt% vs. 36.2 wt%, carbon yield) in the presence of hydrogen at 400 psi.[287] Doping of HZSM-5 with Ce decreased the coke formation, and increased the selectivity of decarbonylation of furfural to form furan and CO in CFP of glucose.[295] Magnesium and boron are also effective additives for finely tuning the acidity of HZSM-5.[296, 297] Doping with magnesium leads to decreases in total acid sites and the ratio of weak sites but an increase in medium-strength-acid sites.[297] Substitution of framework Al with B increases weak acid sites, but the number of strong sites was almost unaffected.[296] Both catalysts showed improved stability in production of olefins from either methanol or pyrolysis vapor.[296, 297]

3.3.2. Other microporous materials

The product distribution of catalytic cracking depends on the type of catalyst used, particularly the shape selectivity and acidity of the catalyst.[49, 298-300] Besides HZSM-5, various microporous materials such as ferrierite, mordenite, β Zeolite, HY, rare-earth Y (REY) zeolite, and silicate were investigated in CFP of biomass. Table 6 summarizes the specifications of those microporous materials other than ZSM-5. Those mircroporous materials differ either in acidity, pore size or pore structure. In general, zeolites of small pore size will not be able to produce any aromatics with oxygenates but only CO, CO_2, and coke.[246] Medium-pore zeolites with pore sizes in the range of 0.52–0.59 nm produced aromatics with high yields, while large-pore zeolites showed low yields to both aromatics and oxygenates and high yields to coke.[246]

By comparing the CFP of glucose over ZSM-5, silicalite, β zeolite, silica-alumina, and Y zeolite, Carlson et al. found that the CFP process is shape selective and the proper catalyst can be found by changing the type of active site and the pore shape.[207] Mihalcik et al. systematically compared the activity of some commercially available acidic zeolites including H-ferrierite, H-mordenite, HY, HZSM-5, and Hβ in CFP of various types of biomass (oak, corn cob, corn stover, and switchgrass) and their fractional components (cellulose, hemicellulose, and lignin).[249] The presence of the acidic zeolites decreased the yield to condensable products and increased the yields to coke and non-condensable gases.[249] Ben and Ragauskas found that the presence of ZSM-5, mordenite, Y zeolite, β zeolite, and ferrierite greatly decreased the content of both aliphatic hydroxyl groups and carboxylic acid groups in bio-oil resulting from CFP of lignin.[301] From the conversion of cyclopentanone on HY, Huang et al. found that relatively weak Brønsted acid sites are able to initiate the conversion of cyclopentanone, and that a larger density of

accessible acid sites promotes the condensation reactions.[302] HY zeolite deactivated less severely than HZSM-5 in the n-heptane transformation.[266] High temperature will lead to thermal distortion of zeolite pore size; ZSM-5 and mordenite were ineffective for the conversion of bulkier monolignols from syringyl lignin due to size exclusion or pore blockage, while β and Y zeolites were very effective for deoxygenation of those lignin-derived oxygenates.[269] Uzun et al. found that ZSM-5 gave the highest liquid yield in CFP of corn stalks among ZSM-5, Ultrastable zeolite Y (USY) and HY catalysts, and HY led to the lowest oxygen content in the resulting bio-oil.[303]

Hβ was more active than HY and H-ferrierite for deoxygenation reactions in CFP of pine wood.[304] Mihalcik et al. found Hβ is the second most active catalyst for aromatic hydrocarbon production from H-ferrierite, H-mordenite, HY, Hβ, and HZSM-5.[249] The product distribution of Hβ varied with feedstock while HZSM-5 converted all feedstock to similar products.[249] Hβ can catalyze decarbonylation, which leads to more CO in gas products.[305] The lower Si/Al ratio of Hβ also led to greater extent of deoxygenation and higher yield to aromatic hydrocarbons in CFP of lignocellulosic biomass.[249] The higher surface density of the Brønsted acid led to lower organic yield and higher water yield due to the cracking ability of Hβ.[306] More coke formed over Hβ than on H-ferrierite, H-mordenite, HY, and HZSM-5.[249] Although the largest amount of aromatic hydrocarbons was produced by HZSM-5, its instantaneous coking was kept to a minimum.[249] H-ferrierite and H-mordenite were found active for pyrolysis vapor conversion due to their framework characteristics associated with the pore system.

Table 6 Specifications of various zeolites investigated in CFP

Type of catalyst	Surface area (m^2/g)	Pore size (nm)	Si/Al ratio	Acidity (mmol NH_3)	Ref.
HY	629	NA	2.6	0.576	247
HY	NA	NA	2.9	0.97	266
HY	119-730	0.74-0.85	2.6-84	NA	155, 210, 240, 299, 303
USY(6.3)	575	NA	3.2	0.407	247
USY(14)	524	NA	7	0.360	247
USY(360)	436	NA	180	0.011	247
USY	520	0.8	7	0.91	307
USY	530	0.74	7	1.2	267
USY	>675	NA	2.75	NA	303
β-zeolite	63	0.7	50	NA	82
β-zeolite	630	NA	NA	0.183	247
β-zeolite	410	0.7	14	1.1	307
Hβ	650	0.66	15	1.1	267
Hβ	589	NA	12.5	0.68	306
Hβ	546	NA	75	0.72	306
Hβ	661	NA	150	0.17	306
H-mordenite	474	NA	45	0.159	247
H-mordenite	112.6	0.67	7-14	NA	155, 299, 307
Ferrierite	347	NA	10	0.326	247
Ferrierite	NA	0.54	10	NA	249

Silicate	401.9	0.54	NA	NA	155, 299
Silicalite	550	0.55	pure	0	267
SAPO-34	441	NA	NA	0.180	247
ZSM-11	149	NA	240	0.136	247
FCC	176	NA	6	NA	212
Natural zeolite	65.42	NA	1.45	NA	208
REY zeolite	>650	NA	88	NA	307

NA: not available

Only very limited amounts of PAH were produced on mordenite zeolite in CFP of pine wood biomass and softwood kraft lignin.[300, 301] Due to size exclusion or pore blockage, the bulkier monolignols derived from syringyl lignin will not be effectively converted by mordenite.[269] ZSM-5 and mordenite facilitated decarboxylation of primary pyrolysis vapors.[301] Y, β, and ferrierite zeolites were more effective for dehydration and decarbonylation than ZSM-5 and mordenite.[301] Y and β zeolites also favored removing methoxyl groups from aromatics.[301] HZSM-5 and silicalite are most selective to gasoline range aromatic hydrocarbons, while H-mordenite and HY catalysts are more selective to kerosene-range hydrocarbons.[155, 299] H-mordenite is also more selective to aromatic hydrocarbons, while HY is more selective to aliphatic hydrocarbons.[155, 208, 303] USY catalysts, especially those of low Si/Al, enhance gasification and also increase the aromatic compounds in product oil in CFP of corn stalks, alkaline lignin, and *Jatropha* waste.[247, 267, 303, 308] However USY showed a fast deactivation in decomposition of polyethylene.[309]

3.4. Mesoporous materials

In porous materials, pore size affects the activity and selectivity of the catalysts in CFP. It controls access to active sites inside the micropores for given reactants. Figure compares the kinetic diameters of biomass feedstock, oxygenates, and hydrocarbons with the zeolite micropore size. Primary pyrolysis products of a kinetic diameter larger or equal to that of glucose would not be able to diffuse into the pores of microporous materials.[246] Thus the pyrolysis of biomass and its primary large products/intermediates will hardly be affected by the presence of microporous materials. However, mesoporous materials with adjustable uniform pore size (2–15 nm) allow the interaction of large organic molecules with the active sites, which could be beneficial especially for *in situ* CFP.[56] The very large pores of mesoporous materials are even able to process large lignocellulosic macromolecules. Table 7 summarizes the basic characterisstics of mesoporous materials tested in CFP.

Aluminosilicate mesoporous MCM-41 has been reported as a good catalyst for cracking vacuum gas oil, recycled plastic wastes such as polyethylene, and naphtha with high selectivity to middle distillate.[310] Acidity of mesoporous materials can be tailored by aluminum incorporation.[310] Twaiq et al. found that CFP of palm oil in the presence of MCM-41 produced about 80 wt% of gasoline, kerosene and diesel range hydrocarbons.[310, 311] However MCM-41 led to higher coke deposition than ZSM-5 and USY zeolites due to its lower acidity and larger pore volume.[310] The CFP of biomass in the presence of siliceous mesoporous MCM-41 induced considerable increase in total liquid products, but it was mainly due to higher water formation, leaving the organic phase almost unaffected.[312] However, the presence of Al-MCM-41 in CFP of spruce wood increased the yield to acetic acid and furans, and lowered the yield to higher molecular-weight phenols.[312, 313] Levoglucosan was almost completely eliminated by Al-MCM-41

in CFP of cellulose.[313] The presence of Al-MCM-41 significantly increased the yield to phenolic compounds in CFP of Lignocel and *Miscanthus* biomass.[56, 314, 315] Decreasing Si/Al ratio increases the number of acidic sites on Al-MCM-41, which should be finely tuned to achieve high yield to desirable products. Moderate steaming of Al-MCM-41 (at 550 and 750°C, 20% steam partial pressure) leads to a decrease in surface area and the number of acid sites, and in turn lowers the liquid products yield; more specifically, it decreases organic phase product yield.[312] Lowering the Si/Al ratio of Al-MCM-41 led to an increase in the yield to high value aromatic compounds.[314] Incorporation of Fe and Cu into Al-MCM-41 led to even higher yield to phenols while doping with Zn led to the lowest yield to phenols but also the lowest coke formation in CFP of *Miscanthus* biomass.[314, 316] However, the MCM-41-type catalysts are not as active as HZSM-5.[250]
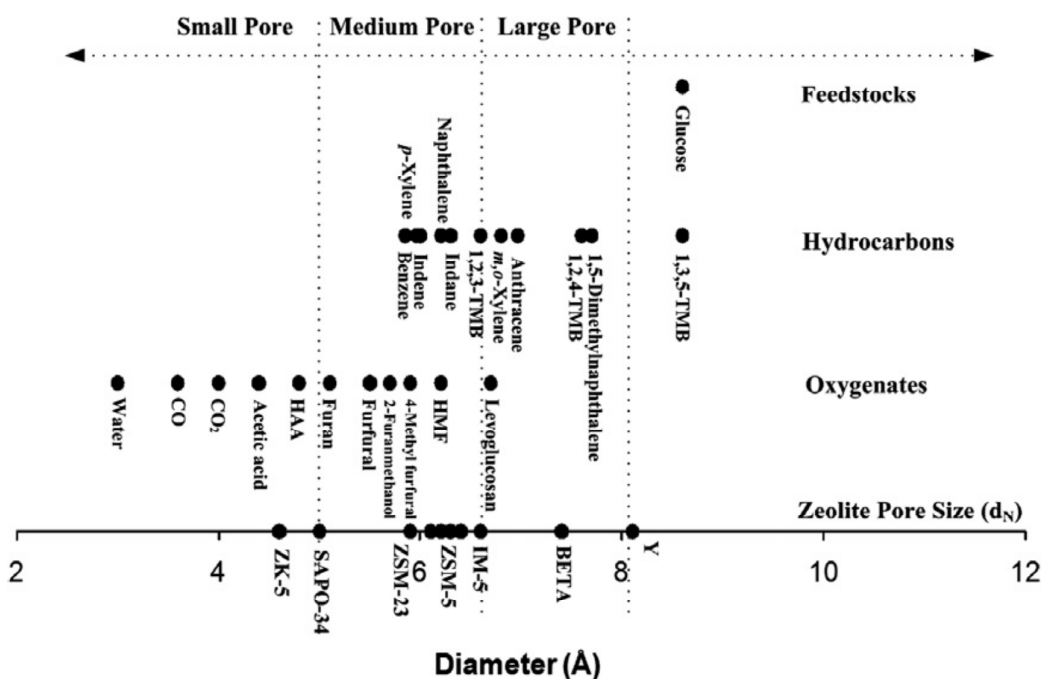

Figure 8 Schematic comparison of zeolite pore diameter and kinetic diameter of feedstocks, oxygenates, and hydrocarbons in CFP of biomass.(Adapted with permission from Jae et al., *J. Catal.*, 2011, **279**, 257-268.[246]. Copyright 2011 Elsevier)

SBA-15 is a highly thermally and hydrothermally stable mesoporous material of highly ordered hexagonally arranged mesochannels, making it suitable catalytic materials.[317] It also has been investigated for application in CFP of biomass.[318] Pure siliceous SBA-15 did not change the organic phase product yields compared to non-catalytic fast pyrolysis.[319] Al-SBA-15 is more active than SBA-15 and led to higher yield to light furans and phenols.[318] Lower Si/Al ratio led to higher catalytic activity.[318] The yield to light phenols increased with decreasing Si/Al ratio at the expense of decreased yield to heavy phenols.[318] Moreover, catalytic cracking in the presence of Al-SBA-15 reduced the yield to light aldehydes and ketones but increased the yield to acetic acid.[318]

MSU-H$_{BEA}$ and MSU-W$_{BEA}$ are more stable than Al-MCM-41 in steaming conditions and are very selective for the formation of PAH and heavy fractions.[320] Almost no acids, alcohols or carbonyls are observed due to the stronger acidity of MSU-H$_{BEA}$ and MSU-W$_{BEA}$.[320] Al-MSU-F, a zeolite-like catalyst with a cellular foam framework of 15 nm pores also selectively reduced all the

oxygenated lignin-derived compounds and concurrently enhanced the formation of aromatic hydrocarbons.[209]

Table 7 Specifications of mesoporous materials tested in CFP

Type of catalyst	Surface area (m^2/g)	Pore size (nm)	Si/Al ratio	Acidity (mmol NH_3)	Ref.
SBA-15	807	6.9	Pure silica	NA	82
SBA-15	698	9.1	Pure silica	NA	210
Al/SBA-15	511	7.2	10	NA	210
MCM-41	1000	3.8	50	NA	82
Al-MCM-41	972	3.3	20.5	NA	314
Al-MCM-41	866	3.3	34.2	NA	
Al-MCM-41	914	3.5	51.3	NA	
Al-MCM-41	990	3.0		0.20	320
Al-MCM-41	950	2.6	20	NA	321
Cu-Al-MCM-41	879	2.3	24	NA	314
Fe-Al-MCM-41	651	2.3	23	NA	
Zn-Al-MCM-41	1298	1.8	49	NA	
Al-MCM-48	1350	2.6	20	NA	321
MSU-S/H$_{BEA}$	1017	3.0	NA	0.20	320
MSU-S/W$_{BEA}$	923	3.5	NA	0.24	
Meso-MFI	567	4.1	15	NA	321
0.5%Pt/Meso-MFI	472	4.1	15	NA	

NA: not available.

3.5. Supported transition metal catalyst

HDO is an efficient way to improve the quality of bio-oil and for the production of hydrocarbon products. Conventional HDO of bio-oil is carried out in liquid phase at 250–450°C with hydrogen pressure ranging from 7.5 to 30 MPa in the presence of conventional sulfide CoMo or NiMo catalysts.[14, 322-325] The high operating pressure of conventional HDO requires a high capital investment and high operational costs, and it is less compatible with fast pyrolysis of biomass. The use of sulfide catalysts requires co-feeding of certain sulfides to maintain its activity which causes other serious problems for the process. Thus, gas-phase HDO that is carried out at atmospheric hydrogen pressure is preferable because it could be more conveniently integrated with a pyrolysis unit. Transition metals supported on acidic supports have been studied exclusively in gas-phase HDO due to their high activity. Olefins, aldehydes, ketones, aliphatic ethers, alcohols, and carboxylic groups are all highly active in HDO in the presence of a catalyst.[35, 194, 326-328] The conversion of aromatic oxygenates such as phenols and phenolic ethers requires more severe reaction conditions, such as higher temperatures.[188, 329]

Sitthisa and Resasco compared the activity of Cu/SiO$_2$, Pd/SiO$_2$, and Ni/SiO$_2$ in vapor-phase HDO of furfural at ambient pressure and 210-290°C.[194] Cu/SiO$_2$ selectively converted furfural into furfuryl alcohol while Pd/SiO$_2$ mainly converted furfural into furan via decarbonylation.[194] Ring opening was obtained in significant amounts, and led to butanal, butanol, and butane over Ni/SiO$_2$.[194] Ni/SiO$_2$ was tested in gas-phase HDO of phenol.[189, 330] It was found that direct hydrogenolysis of phenol to benzene was favored with high Ni loading and elevated temperatures

while the selectivity strongly depended on water content.[326, 327] Higher water content led to higher ring saturation. Sitthisa et al. then developed Pd-Cu/SiO$_2$ and compared it with Pd/SiO$_2$ in the vapor-phase HDO of furfural and 2-methylpentanal at atmospheric pressure and 210–250°C.[328] Both catalysts showed high hydrogenation activity but Pd-Cu/SiO$_2$ was much more active than Pd/SiO$_2$. Pentane is the main product from 2-methylpentanal via decarbonylation at low space times while di-methylpentyl ether dominated at higher space times due to etherification. Addition of Cu to Pd leads to the formation of a Pd-Cu alloy that suppresses the decarbonylation activity and improves the hydrogenation and etherification activity.[328] However, the only decarbonylation product formed was furan regardless of the temperature and space time employed because the aromatic ring inhibited the formation of alkoxide surface intermediates, which is required for etherification.[328] Density functional theory study of furfural conversion to furan, furfuryl alcohol, and 2-methylfuran on Pd(111) indicates that thermodynamics favors the production of furan and CO from furfural while the activation energy for furfural reduction to furfuryl alcohol is lower than that for its decarbonylation to furan.[331] Olcese et al. found that Fe/SiO$_2$ showed high HDO selectivity in vapor-phase HDO of guaiacol over a wide range of temperatures.[332] Benzene and toluene are selectively produced, and the highest benzene/toluene yield of 38% was achieved at 74% conversion.[332] Sun et al. studied carbon-supported metal catalysts including Cu/C, Fe/C, Pd/C, Pt/C, Ru/C, and PdFe/C in vapor-phase HDO of guaiacol.[193] All those carbon-supported metal catalysts are capable of catalyzing the HDO of guaiacol, and phenol was found to be the major intermediate over all catalysts.[193] The noble metals favor the saturation of aromatic rings to form cyclohexanone and cyclohexanol, followed by ring opening to form gaseous products. Base metals showed lower activity than noble metals but high selectivity to form benzene along with small amounts of toluene and trimethylbenzene, leaving the aromatic ring untouched. This is desirable for HDO since it minimizes the hydrogen consumption for sufficient oxygen removal.[193] A bimetallic PdFe/C catalyst exhibited significantly higher HDO activity compared to monometallic counterparts due to the modification of Fe by Pd.[193] The highest aromatic hydrocarbon (benzene/toluene/trimethylbenzene) yield of 83.2% was achieved on PdFe/C at 450°C.[193] Lu et al. studied the *in situ* CFP of poplar wood in the presence of Pd/SBA-15 with a Py-GC/MS system.[329] Pd/SBA-15 had exceptional capability to crack the lignin-derived oligomers to monomeric phenolic compounds and further convert them to phenols without the carbonyl group and unsaturated side chain.[329] Anhydrosugars are almost completely eliminated, and the furan compounds are decarbonylated in the presence of Pd/SBA-15.[329] Linear aldehydes and ketones are significantly reduced.[329] The activity of Pd/SBA-15 increased with increasing Pd loading from 0.79 wt% to 3.01 wt%.[329]

Runnebaum et al. found that the conversion of furan over Pt/γ-Al$_2$O$_3$ at 300°C and 140 kPa led to the formation of C$_3$–C$_4$ aliphatic hydrocarbons and some gasoline-range C$_7$ aliphatic hydrocarbons.[333] González-Borja and Resasco tested the activity of carbon nanofiber-supported Pt, Sn, and Pt-Sn catalysts coated on Inconel monoliths for vapor-phase HDO of anisole and guaiacol at atmospheric pressure and 400°C.[188] Both supported monometallic and bimetallic catalysts are active in HDO reactions, and the bimetallic Pt-Sn catalyst showed much higher stability and activity than the monometallic Pt and Sn catalysts.[188] The main products obtained from guaiacol and anisole are phenol and benzene, while oxygen was removed as methanol and water.[188] Nimmanwudipong et al. studied the vapor-phase HDO of guaiacol on Pt/γ-Al$_2$O$_3$ at 300°C and 140 kPa.[334] Anisole and phenol were formed as primary products via HDO as the aromatic C-O

bond in guaiacol was broken in presence of H_2.[334] Phenol, catechol, and 3-methylcatechol are the predominant products over Pt/γ-Al_2O_3.[334] Benzene, toluene, anisole, cyclohexanone, 2-methylphenol, 2-methyoxy-3-methylephenol, 6-methylguaiacol, and 1,2-dimethyoxybenzene are found in smaller amounts.[334] The vapor-phase conversion of anisole over Pt/γ-Al_2O_3 at 300°C and 140 kPa led to selective production of phenol and methane, which is kinetically significant.[335] All other primary products were apparently produced by transalkylation of methyl groups.[335, 336] 2-methylphenol and benzene were the second most abundant products.[336] Selective removal of oxygen from compounds like anisole requires both an active hydrogenation catalyst and higher H_2 partial pressure.[335] Nimmanwudipong et al. also studied Pt/MgO in vapor-phase HDO of guaiacol under the same conditions. Pt/MgO was more selective to HDO reactions than Pt/γ-Al_2O_3 because the acid catalyzed transalkylations were avoided.[192] The selectivity to phenol on Pt/MgO is about twice that on Pt/γ-Al_2O_3 at the expense of catechol selectivity. [192]

By comparing the vapor-phase HDO of 4-methylanisole over Pt/γ-Al_2O_3, and Pt/SiO_2-Al_2O_3 in the presence of H_2 at 300°C, Runnebaum et al. found that Pt/SiO_2-Al_2O_3 is three times more active than Pt/γ-Al_2O_3.[337] Foster et al. also found Pt/SiO_2 to be more active than Pt/γ-Al_2O_3 in vapor-phase HDO of m-cresol at 260°C.[338] Toluene is selectively produced on both catalysts with methylcyclohexanol and methylcylohexane as the two second most abundant products.[338] The very weak acidic hydroxyl groups on the silica surface are believed to dehydrate the unsaturated alcohol intermediates formed by hydrogenation of m-cresol, and the increased mobility of phenolic species on the silica surface relative to alumina improves the HDO rate of m-cresol on Pt/SiO_2.[338] More interestingly, the activity of Pt/γ-Al_2O_3 changed drastically when the acidity of γ-Al_2O_3 was modified by K_2CO_3 and NH_4F.[338] Enhancing the acidity of γ-Al_2O_3 by NH_4F increases the overall HDO rate while the treatment with K_2CO_3 decreases it.[338] This suggests certain synergic effects between the metal and acid functions of the catalyst in the HDO reaction. [338] In the vapor-phase HDO of cresol on Pt/γ-Al_2O_3 , Zanuttini et al. found the yield to toluene, benzene, and methylcyclohexane also depends on reaction conditions such as the metal loading, the H_2/cresol ratio and the reaction temperature.[339] Toluene hydrogenation to methylcylohexane is favored at low reaction temperature and the yield to toluene reached a maximum at about 300°C.[339] Higher temperature leads to the demethylation of toluene to benzene.[339] Zhu et al. found Pt/Hβ was capable of catalyzing the transalkylation and HDO of anisole at 400°C and atmospheric pressure.[190, 261] Both transalkylation and HDO rates were higher than corresponding monofunctional catalysts. Benzene, toluene, and xylenes were produced as main products.

4.   Practical CFP of lignocellulosic biomass

Catalytic fast pyrolysis has been extensively investigated in the past two decades using either various model compounds and/or biomass feedstock over a wide range of catalysts. Most of the research results are summarized in Table 8 along with the catalysts, reaction conditions and feedstock. The studies with model compounds showed that small oxygenates can be readily converted into aromatic hydrocarbons over ZSM-5-based catalysts.[256] Furans, furfurals, and glucose can also be converted into aromatic hydrocarbons over ZSM-5 under proper reaction conditions.[50, 156, 207, 243, 265, 274] However, phenols are much more recalcitrant and require higher reaction temperature.[82, 256] The CFP of alkaline lignin over HZSM-5 catalysts of various Si/Al ratios indicates higher acidity leads to higher yield to aromatic hydrocarbons.[267] Hβ and USY are also efficient catalysts for CFP of alkaline lignin; USY showed the higher lignin conversion and aromatic hydrocarbon yield along with the lowest char yield.[267] This suggests that relatively

larger micropores are more favorable for phenol conversion. The CFP of biomass feedstock such as pinewood, rice husk, and corncob showed relatively low hydrocarbon yields although the non-phenolic oxygenates have been greatly reduced.[340] It is worth note that hierarchical ZSM-5 modified by 1% Ga led to high yields to both bio-oil and hydrocarbons in CFP of Radiata pine sawdust at mild temperature (Table 8).[340]

The main purpose of the catalyst in both *in situ* and *ex situ* CFP is removing the oxygenated compounds and catalytically cracking the high-molecular-weight compounds into products of desired carbon chain length. Generally, any solid catalyst for CFP of biomass can operate either way. For *in situ* CFP, catalyst and biomass feed were intimately mixed in the pyrolysis reactor, which enables immediate contact between the pyrolysis vapor and catalyst. Thus the catalysts can intervene in the pyrolysis and cracking process of biomass at an earlier stage. This could enhance the decomposition of larger pyrolysis fragments or oligomers with proper catalysts and in turn reduce the possibility of re-polymerization of primary pyrolysis products. *In situ* CFP also removes/upgrades the active components as soon as they are generated. This reduces the chance of secondary char formation, and could potentially increase the yield to desirable products. From an engineering point of view, *in situ* CFP simplifies the process and also offers a better chance to integrate the reaction heat of pyrolysis with that of the upgrading reactions. However, the very short residence time (1–2 s) of the pyrolysis vapor may only remove the most active components and limit the deoxygenation degree of bio-oils. Thus it can only partially improve the bio-oil quality but it would be beneficial for subsequent upgrading operations such as hydroprocessing. A large catalyst-to-biomass ratio is necessary to ensure a higher degree of upgrading and higher yield to liquid hydrocarbon products. The high catalyst-to-biomass ratio will reduce the effective volume of the pyrolysis reactor and in turn decrease the efficiency of the reactor. Despite the simplicity of *in situ* CFP, the pyrolysis temperature and upgrading/cracking temperature must be identical due to the reactor configuration. That would compromise the optimal respective reaction temperatures of pyrolysis and upgrading. It also increases the difficulty of separating char as a solid product due to its being mixed with the catalysts.

For *ex situ* CFP, the upgrading/cracking operation can run under independent conditions. It is more flexible to operate under respective optimal reaction conditions such as reaction temperature and residence time for each step.[136] Also, char formed in the fast pyrolysis process can be separated by proper hot vapor separation/filtration. The obtained char could be a valuable solid product. Despite the high flexibility in choosing operating conditions, *ex situ* CFP requires more reactors and a longer process, which leads to substantially higher fixed assets investment and operation cost. The process integration degree will be inferior to that of *in situ* CFP. Despite the long list of questions and uncertainty regarding *in situ* and *ex situ* CFP, only very little work has been done with respect to those concerns.[40] Nguyen et al. proposed using the degree of oxygen removal (Eq.(0)) to justify *in situ* versus *ex situ* CFP where $Y_{\text{bio oil}}$ is the weight yield to bio oil, $x_{\text{Oxy in bio oil}}$ and $x_{\text{Oxy in biomass}}$ are the oxygen weight percentage in bio oil and biomass, respectively.[341] However, oxygen removal degree alone is not sufficient to justify either of the processes since very low bio-oil yield with high oxygen content in bio-oil can also lead to a high oxygen removal degree number. At a minimum, bio-oil yield should be provided along with oxygen removal degree for adequate justification of a process.

$$\text{Oxygen removal degree} = \left[1 - \frac{x_{\text{Oxy in bio oil}} \times Y_{\text{bio oil}}}{x_{\text{Oxy in biomass}}} \right] \times 100 \tag{0}$$

Güngör et al compared the *in situ* and *ex situ* CFP of pine bark over ReUS-Y.[342] The *in situ* CFP reaches its highest bio-oil yield (9.3 wt%) at lower temperature (500°C) while *ex situ* CFP requires 600°C to reach the same bio-oil yield.[342] *In situ* CFP led to more low-molecular-weight lignin.[342] It seems that the *in situ* CFP lowered the decomposition temperature of lignin fragments and the catalyst intervened in the pyrolysis process of biomass at an earlier stage. Yildiz et al. further compared *in situ* and *ex situ* CFP of pine wood on a continuously operated mini-plant with ZSM-5 catalyst.[40] Both *in situ* and *ex situ* CFP led to effective oxygen removal and the conversion of high-molecular-weight compounds to lower ones. A significant decrease (2.3 wt%) of char yield for *in situ* mode was observed, although the authors ascribe it to higher ratio of heat carrier to biomass. For *ex situ* CFP, the decrease of char yield is almost marginal (0.2 wt%) compared to the non-catalytic pyrolysis process. *In situ* CFP led to a higher yield to gas products than *ex situ* CFP (26.2 wt% vs. 23.9 wt%), while the *ex situ* CFP led to higher coke deposition (10.1 wt% vs. 9.7 wt%) and coke formation (15.7 wt% vs. 13.6wt %).[40] However, the organic liquid yields in both cases are similar and lower than that obtained from non-catalytic fast pyrolysis. More interesting is the observation that *in situ* CFP also resulted in much higher selectivity to phenols and aromatic hydrocarbons.

Table 8 Summary of the catalysts, reaction conditions, and results in research on catalytic fast pyrolysis of biomass

Feed	Reaction conditions				Results			
	Catalyst	Temp, °C	WHSV g_oil/ g_cat/h	Process type	Bio-oil Yield, wt%	Hydrocarbon Yield, wt%	Product quality and oxygen content, wt%	Ref
Synthetic bio-oil	HZSM-5	330-410	3.6	*ex situ*[1]	NA	31.8	85.9% conversion, equal amounts of aliphatic and aromatic hydrocarbons; O = 12.5	256
Kraft lignin	HZSM-5	500-650	NA	*in situ*[1]	NA	2.0-5.2	Mainly BTX	273
Alkaline lignin	NaZSM-5	650	NA	*in situ*[1]	55.2	6.0	Mainly phenols	267
	Silicalite	650	NA		53.2	3.6	Mainly phenols	
	HZSM-5(210)	650	NA		51.7	8.4	Mainly phenols	
	HZSM-5(55)	650	NA		56.5	21.3	Dominant aromatic hydrocarbons	
	HZSM-5(25)	650	NA		58.2	31.1	Dominant aromatic hydrocarbons	
	HZSM-5(15)	650	NA		57.1	33.8	Dominant aromatic hydrocarbons	
	Hβ	650	NA		60.0	34.0	Dominant aromatic hydrocarbons	
	USY	650	NA		74.9	39.2	Dominant aromatic hydrocarbons	
Maple wood pyrolysis bio-oil	HZSM-5	290-410	1.8, 3.6	*ex situ*[1]	NA	27.9	Mainly aromatic hydrocarbons	155
	HY				NA	18.9	Mainly aliphatic hydrocarbons.	
Wood bio-oils	HZSM-5	410-490	3.5, 7.0	*ex situ*[1]	15.1-23.4	NA	Mainly aromatic hydrocarbons	251
Pinewood	Hβ	400-440	NA	*in situ*[2]	26.0	NA	Mainly oxygenates, O = 32.2	305
Pinewood sawdust	HZSM-5	600	0.5	*in situ*[2]	NA	14%[4]	Dominant aromatic hydrocarbons	278
Pinewood sawdust	HZSM-5	400-500	NA	*in situ*[3]	NA	18.9	O = 18.6	343
Pinewood sawdust	Ga/ZSM-5	550	0.35	*in situ*[2]	NA	21.6%[4]	Dominant aromatic hydrocarbons	50
Pinewood sawdust + alcohols	HZSM-5	450	0.56	*in situ*[2]	NA	15.6-21.1%[4]	Dominant aromatic hydrocarbons	285

Pine wood	Na$_2$CO$_3$/Al$_2$O$_3$	500	NA	*ex situ*[1]	9	NA	Almost completely removed acids, but higher carbonyl components in bio-oil, O = 12.3	344
Radiata pine sawdust	HZSM-5	450-550	4	*ex situ*[1]	43.7	12.8	Mainly aromatic hydrocarbons	292, 345
	HY		8		45.7	NA	Almost no aromatic hydrocarbon	345
	Ga/HZSM-5		4		51.3	23.4	Mainly aromatic hydrocarbons	292, 345
Radiata pine sawdust	HZSM-5	500	NA	*ex situ*[1]	46.6	12.5	Largely reduced non-phenolic oxygenates, most phenols remained	340
	MMZ$_{ZSM-5}$		NA		50.6	1.0	Phenols remain intact, other oxygenates lower	
	Meso-MFI		NA		42.9	14.2	Largely reduced non-phenolic oxygenates and also lowered phenols, with high aromatics yield	
	1%Ga/ Meso-MFI		NA		45.9	19.6	Largely reduced non-phenolic oxygenates and also lowered phenols, with higher aromatics yield	
	5%Ga/ Meso-MFI		NA		NA	NA	Similar to HZSM-5, inferior to 1% Ga/Meso-MFI	
Rice husk	Meso-MFI	500	NA	*ex situ*[1]	NA	NA	Decreased oxygen content, increased aromatic hydrocarbon and light phenols, with levoglucosan completely decomposed; Pt enhanced the activity	346
	Pt- Meso-MFI		NA		NA	NA		346
Rice husk	HZSM-5	500-550	NA	*ex situ*[1]	4.4	NA	Mainly aromatic hydrocarbons, O = 8.1	257
Rice stalk	ZSM-5	550	NA	*in situ*[2]	NA	12.8%[4]	Dominant BTX along with 10.5% olefin yield.	347
Corncob	HZSM-5	550	NA	*in situ*[2]	13.7	10.17	Dominant aromatic hydrocarbons, O = 14.69	259
Corncob	Fresh/Spent FCC catalyst	550	NA	*in situ*[2]	16-23%[4]	NA	Mainly oxygenates, O = 16.0 -17.6	348

Corn stalks	ZSM-5	500	NA	*in situ*[1]	NA	27.55	O = 20.23	303
	USY		NA		NA	22.2	O = 15.70	303
	HY		NA		NA	26.1	O = 19.98	303
Wood mixture	HZSM-5	500-550	1.05-1.14	*ex situ*[1]	5.5	NA	High aromatic hydrocarbon; O = 4.7	258
Wood	Hβ(Si/Al=12.5, 75, 150)	450	NA	*in situ*[2]	12.3-17.0	NA	Mainly oxygenates, stronger acidity results in more water and PAH	349
Hybrid poplar wood	HZSM-5	450-500	NA	*in situ*[2]	33.6	NA	Mainly oxygenates; O = 21.9	350
White oak	Ca/Y zeolite	500	NA	*in situ*[2]	30	NA	Dominant oxygenates; O = 17.9	351
	β zeolite	500	NA		29	NA	Dominant oxygenates; O = 17.0	
Cottonseed cake	Clinoptilolite	550	NA	*in situ*[1]	30.84	NA	O = 14.33	352
Rapeseed cake	HZSM-5, Hβ	400	NA	*ex situ*[1]	10.4-13.4	NA	Similar amounts of aliphatic and aromatic hydrocarbons: O = 21.35-28.23	353
Jatropha wastes	HZSM-5	550	NA	*ex situ*[1]	4.1-8.7	NA	76.7-96.4% conversion, products mainly aromatic hydrocarbons	247
Particle board	HZSM-5	500	NA	*ex situ*[1]	42.54	7.8	Oxygenates are dominant	354
	Ga/HZSM-5		NA		46.27	10.0	Oxygenates are dominant	
	Hβ		NA		44.60	5.4	Oxygenates are dominant, but levoglucosan completely decomposed	

O: oxygen content, wt%; [1] packed bed reactor; [2] fluidized bed reactor; [3] conical spouted-bed; [4] carbon yield

5. Conclusion and perspective

Lignocellulosic biomass has the characteristics of high oxygen content, and so are the resulting liquid products produced by conventional fast pyrolysis processes. To produce high quality liquid transportation fuels from lignocellulosic biomass, efficient removal of oxygen from the feedstock is required. CFP is one of the most promising techniques with the potential to meet this goal. Either the *in situ* or *ex situ* catalytic upgrading technique could be integrated with fast pyrolysis and lead to novel CFP processes. Catalyst development is the key for the process innovation. Improving the design of the catalyst requires better understanding of the thermal decomposition chemistry and kinetics of the biopolymers of lignocellulose and better understanding of what intermediate components are to be dealt with.

Generally, according to the oxygenated functional groups of the intermediates identified, reactions such as decarbonylation, decarboxylation, dehydration, hydrogenation, and ketonization/condensation could be employed to remove the oxygen and to produce hydrocarbons with the desired carbon backbone. It is highly desirable to remove as much oxygen as possible in the form of CO_2, which preserves most of the hydrogen of the biomass in bio-oil products. The ideal products from CFP of biomass are the transportation-fuel-range hydrocarbons. However, it is often difficult to achieve such goals in one simple step, especially with high yields towards desired products. Efficient removal of the most active and detrimental components while producing more stable bio-oil with high yield for subsequent refining could be a more feasible route.

As is known, the inorganics have a remarkable influence on the pyrolysis of lignocellulose, which could either affect the structure of lignocellulose and/or interfere with the reaction pathways of lignocellulose pyrolysis.[215] Since it would be impossible for a heterogeneous catalyst to catalyze the thermal decomposition of lignocellulose, exploiting a soluble catalyst that could be impregnated into the biomass feedstock seems to be the only possibility for catalytically controlling the initial decomposition process of biomass and to decompose the biomass in a selective way if possible.

Because fast pyrolysis of biomass produces large amounts of water, it is desirable to remove the most problematic small components such as formic acid, acetic acid, and small molecular aldehydes and ketones by steam reforming.[200, 202, 204, 355] Thus the content of both the small oxygenates and water could be reduced and oxygen will be rejected mainly as carbon oxides. The *in situ*-generated hydrogen could be utilized for certain hydrogenation or HDO of other components, which would also help preserve hydrogen in the products if proper hydrogenation active sites could be incorporated.

Although HDO and steam reforming could improve the quality of bio-oils by converting the most problematic small oxygenates into less harmful compounds, they are not able to maximize the carbon yield to gasoline- or diesel-range products. To achieve higher transportation fuel yield and to make the best use of the abundant carboxylic and carbonyl components, ketonization of carboxylic acids as well as aldol condensation of ketones and aldehydes should be addressed.[163-170] Metal oxides, which provide large varieties of acid and base properties differing in strength and/or nature, are the most promising catalysts for this purpose. Their properties and structures can be finely tuned by doping or combining with other metal oxides, or they can be dispersed onto proper supports to achieve high activity and selectivity toward the desirable products. Metal oxides merit more investigation to generate insights and nail down the optimal strength and density of active sites, to determine the best composition and structure of the mixed oxides, and to improve the

stability and tolerance to CO_2 and steam conditions in CFP of biomass.

Catalysts need to be developed to facilitate tailored reaction routes toward the desirable products, e.g., via shape selectivity control. The proper catalysts should be capable of catalyzing a wide variety of desired reactions, such as dehydration, hydrogenation, decarbonylation, decarboxylation, C-C coupling, and cracking. Catalysts could be developed with proper acid-base properties designated for proposed products via specific reaction pathways. The stability of the catalyst under fast pyrolysis conditions should also be addressed. Multi-functional catalysts of optimized structure and pore size, proper metal and appropriate acid-base sites to catalyze a sequence of reactions such as hydrogen transfer reactions, HDO, selective hydrogenation, water-gas shift reactions and steam reforming, if necessary, are also desired.

Acknowledgements

References

1.   I. E. Agency, OECD/IEA, 2012 edn., 2012.

2.   J. J. Conti and P. D. Holtberg, U.S. Energy Information Administration, 2011, p. 207.

3.   G. Centi, P. Lanzafame and S. Perathoner, *Catal. Today*, 2011, **167**, 14-30.

4.   J. J. Conti and P. D. Holtberg, U.S. Energy Information Administration, 2013, p. 59.

5.   J. R. Regalbuto, *Science*, 2009, **325**, 822-824.

6.   R. P. Anex, A. Aden, F. K. Kazi, J. Fortman, R. M. Swanson, M. M. Wright, J. A. Satrio, R. C. Brown, D. E. Daugaard, A. Platon, G. Kothandaraman, D. D. Hsu and A. Dutta, *Fuel*, 2010, **89, Supplement 1**, S29-S35.

7.   N. H. Leibbrandt, J. H. Knoetze and J. F. Gorgens, *Biomass & Bioenergy*, 2011, **35**, 2117-2126.

8.   J. C. Serrano-Ruiz and J. A. Dumesic, in *Catalysis for Alternative Energy Generation*, eds. L. Guczi and A. Erdôhelyi, Springer, 2012, p. 536.

9.   D. C. Elliott, E. G. Baker, D. Beckman, Y. Solantausta, V. Tolenhiemo, S. B. Gevert, C. Hornell, A. Ostman and B. Kjellstrom, *Biomass*, 1990, **22**, 251-269.

10.   P. M. Mortensen, J. D. Grunwaldt, P. A. Jensen, K. G. Knudsen and A. D. Jensen, *Appl. Catal., A*, 2011, **407**, 1-19.

11.   R. Agrawal and N. R. Singh, *AlChE J.*, 2009, **55**, 1898-1905.

12.   E. Butler, G. Devlin, D. Meier and K. McDonnell, *Renewable and Sustainable Energy Reviews*, 2011, **15**, 4171-4186.

13.   *Envergent Technologies*, http://www.envergenttech.com/index.php, Accessed 2014.2.15, 2014.

14.   R. H. Venderbosch and W. Prins, *Biofuels, Bioproducts and Biorefining*, 2010, **4**, 178-208.

15.   J. Zhang, H. Toghiani, D. Mohan, C. U. Pittman and R. K. Toghiani, *Energ. Fuel*, 2007, **21**, 2373-2385.

16.   J. C. Hicks, *The Journal of Physical Chemistry Letters*, 2011, **2**, 2280-2287.

17.   D. E. Resasco, *The Journal of Physical Chemistry Letters*, 2011, **2**, 2294-2295.

18.   S. Czernik and A. V. Bridgwater, *Energ. Fuel*, 2004, **18**, 590-598.

19.   D. Mohan, C. U. Pittman and P. H. Steele, *Energ. Fuel*, 2006, **20**, 848-889.

20.   T. Dickerson and J. Soria, *Energies*, 2013, **6**, 514-538.

21.   Y.-T. Cheng and G. W. Huber, *Acs Catal.*, 2011, **1**, 611-628.

22.   C. E. Greenhalf, D. J. Nowakowski, A. B. Harms, J. O. Titiloye and A. V. Bridgwater, *Fuel*, 2013, **108**, 216-230.

23.   G. W. Huber, S. Iborra and A. Corma, *Chem. Rev.*, 2006, **106**, 4044-4098.

24.   D. C. Elliott, T. R. Hart, G. G. Neuenschwander, L. J. Rotness, M. V. Olarte, A. H. Zacher and Y. Solantausta, *Energ. Fuel*, 2012, **26**, 3891-3896.

25.   Q. Zhang, J. Chang, T. Wang and Y. Xu, *Energy Convers. Manage.*, 2007, **48**, 87-92.

26.   J. P. Diebold, *A Review of the Chemical and Physical Mechanisms of the Storage Stability of Fast Pyrolysis Bio-Oils*, http://www.nrel.gov/docs/fy00osti/27613.pdf.

27.   S. Czernik, D. K. Johnson and S. Black, *Biomass Bioenergy*, 1994, **7**, 187-192.

28.   C. Liu and Y. Wang, *Chapter 13. Biofuel and bio-oil upgrading in Biomass Processing, Conversion and Biorefinery*, Nova Science Publishers, 2013.

29.   A. V. Bridgwater, *Environmental Progress & Sustainable Energy*, 2012, **31**, 261-268.

30.   A. V. Bridgwater, *Biomass Bioenergy*, 2012, **38**, 68-94.

31. Y. Zhang, T. R. Brown, G. Hu and R. C. Brown, *Chem. Eng. J.*, 2013, **225**, 895-904.

32. T. P. Vispute, H. Y. Zhang, A. Sanna, R. Xiao and G. W. Huber, *Science*, 2010, **330**, 1222-1227.

33. S. B. Jones, C. Valkenburg, C. W. Walton, D. C. Elliott, J. E. Holladay, D. J. Stevens, C. Kinchin and S. Czernik, *Production of gasoline and diesel from biomass via fast pyrolysis, hydrotreating and hydrocracking: a design case*, Pacific Northwest National Laboratory Richland, WA, 2009.

34. J. Biswas and I. E. Maxwell, *Appl. Catal.*, 1990, **63**, 197-258.

35. D. C. Elliott, *Energ. Fuel*, 2007, **21**, 1792-1815.

36. H. Wang, J. Male and Y. Wang, *Acs Catal.*, 2013, **3**, 1047-1070.

37. M. Saidi, F. Samimi, D. Karimipourfard, T. Nimmanwudipong, B. C. Gates and M. R. Rahimpour, *Energ. Environ. Sci.*, 2014, **7**, 103-129.

38. D. D. Laskar, B. Yang, H. Wang and J. Lee, *Biofuels, Bioproducts and Biorefining*, 2013, **7**, 602-626.

39. T. R. Brown, Y. Zhang, G. Hu and R. C. Brown, *Biofuels, Bioproducts and Biorefining*, 2012, **6**, 73-87.

40. G. Yildiz, M. Pronk, M. Djokic, K. M. van Geem, F. Ronsse, R. van Duren and W. Prins, *J. Anal. Appl. Pyrolysis*, 2013, **103**, 343-351.

41. E. Taarning, C. M. Osmundsen, X. Yang, B. Voss, S. I. Andersen and C. H. Christensen, *Energ. Environ. Sci.*, 2011, **4**, 793-804.

42. M. Ringer, V. Putsche and J. Scahill, *Large-scale pyrolysis oil production: a technology assessment and economic analysis* NREL/TP-510-37779, NREL, 2006.

43. C.-H. Zhou, X. Xia, C.-X. Lin, D.-S. Tong and J. Beltramini, *Chem. Soc. Rev.*, 2011, **40**, 5588-5617.

44. A. Demirbas, *Applied Energy*, 2011, **88**, 17-28.

45. P. Grange, E. Laurent, R. Maggi, A. Centeno and B. Delmon, *Catal. Today*, 1996, **29**, 297-301.

46. O. D. Mante, F. A. Agblevor, S. T. Oyama and R. McClung, *Bioresour. Technol.*, 2012, **111**, 482-490.

47. Y. C. Lin and G. W. Huber, *Energ. Environ. Sci.*, 2009, **2**, 68-80.

48. M. Biddy, A. Dutta, S. Jones and A. Meyer, *In-situ catalytic fast pyrolysis technology pathway*, National Renewable Energy Laboratory & Pacific Northwest National Laboratory, 2013.

49. T. R. Carlson, G. A. Tompsett, W. C. Conner and G. W. Huber, *Top. Catal.*, 2009, **52**, 241-252.

50. Y.-T. Cheng, J. Jae, J. Shi, W. Fan and G. W. Huber, *Angew. Chem.*, 2012, **124**, 1416-1419.

51. T. Mochizuki, S.-Y. Chen, M. Toba and Y. Yoshimura, *Appl. Catal., B*, 2014, **146**, 237-243.

52. S. Tan, Z. Zhang, J. Sun and Q. Wang, *Chinese Journal of Catalysis*, 2013, **34**, 641-650.

53. D. A. Bulushev and J. R. H. Ross, *Catal. Today*, 2011, **171**, 1-13.

54. W. N. R. W. Isahak, M. W. M. Hisham, M. A. Yarmo and T.-y. Yun Hin, *Renewable and Sustainable Energy Reviews*, 2012, **16**, 5910-5923.

55. J.-P. Lange, *Biofuels, Bioproducts and Biorefining*, 2007, **1**, 39-48.

56. M. Stöcker, *Angew. Chem. Int. Ed.*, 2008, **47**, 9200-9211.

57. E. M. Rubin, *Nature*, 2008, **454**, 841-845.

58. D. Klemm, H.-P. Schmauder and T. Heinze, in *Biopolymers Online*, Wiley-VCH Verlag GmbH & Co. KGaA, 2005.

59. D. Klemm, B. Heublein, H.-P. Fink and A. Bohn, *Angew. Chem. Int. Ed.*, 2005, **44**, 3358-3393.

60. L. Ma, T. Wang, Q. Liu, X. Zhang, W. Ma and Q. Zhang, *Biotechnol. Adv.*, 2012, **30**, 859-873.

61. S. Dumitriu, *Polysaccharides: structural diversity and functional versatility*, CRC Press, 2005.

62. M. Balat, *Energy Sources, Part A: Recovery, Utilization, and Environmental Effects*, 2008, **30**, 620-635.

63. F. G. Calvo-Flores and J. A. Dobado, *ChemSusChem*, 2010, **3**, 1227-1235.

64. A. V. Bridgwater, *J. Anal. Appl. Pyrolysis*, 1999, **51**, 3-22.

65. G. Várhegyi, M. J. Antal Jr, E. Jakab and P. Szabó, *J. Anal. Appl. Pyrolysis*, 1997, **42**, 73-87.

66. N. Prakash and T. Karunanithi, *Journal of Applied Sciences Research*, 2008, **4**, 1627-1636.

67. M. S. Mettler, A. D. Paulsen, D. G. Vlachos and P. J. Dauenhauer, *Energ. Environ. Sci.*, 2012, **5**, 7864-7868.

68. A. G. W. Bradbury, Y. Sakai and F. Shafizadeh, *J. Appl. Polym. Sci.*, 1979, **23**, 3271-3280.

69. Y.-C. Lin, J. Cho, G. A. Tompsett, P. R. Westmoreland and G. W. Huber, *J. Phys. Chem. C*, 2009, **113**, 20097-20107.

70. Z. Luo, S. Wang, Y. Liao and K. Cen, *Ind. Eng. Chem. Res.*, 2004, **43**, 5605-5610.

71. I. Milosavljevic, V. Oja and E. M. Suuberg, *Ind. Eng. Chem. Res.*, 1996, **35**, 653-662.

72. A. D. Paulsen, M. S. Mettler, D. G. Vlachos and P. J. Dauenhauer, *Energ. Fuel*, 2013.

73. J. Piskorz, D. Radlein and D. S. Scott, *J. Anal. Appl. Pyrolysis*, 1986, **9**, 121-137.

74. M. S. Mettler, S. H. Mushrif, A. D. Paulsen, A. D. Javadekar, D. G. Vlachos and P. J. Dauenhauer, *Energ. Environ. Sci.*, 2012, **5**, 5414-5424.

75. D. K. Shen and S. Gu, *Bioresour. Technol.*, 2009, **100**, 6496-6504.

76. S. Wang, X. Guo, T. Liang, Y. Zhou and Z. Luo, *Bioresour. Technol.*, 2012, **104**, 722-728.

77. H. Yang, R. Yan, H. Chen, D. H. Lee and C. Zheng, *Fuel*, 2007, **86**, 1781-1788.

78. P. R. Patwardhan, R. C. Brown and B. H. Shanks, *ChemSusChem*, 2011, **4**, 636-643.

79. Y. Peng and S. Wu, *J. Anal. Appl. Pyrolysis*, 2010, **88**, 134-139.

80. D. K. Shen, S. Gu and A. V. Bridgwater, *J. Anal. Appl. Pyrolysis*, 2010, **87**, 199-206.

81. P. Giudicianni, G. Cardone and R. Ragucci, *J. Anal. Appl. Pyrolysis*, 2013, **100**, 213-222.

82. Y. Zhao, L. Deng, B. Liao, Y. Fu and Q.-X. Guo, *Energ. Fuel*, 2010, **24**, 5735-5740.

83. M. A. Serio, S. Charpenay, R. Bassilakis and P. R. Solomon, *Biomass Bioenergy*, 1994, **7**, 107-124.

84. Q. Liu, S. Wang, Y. Zheng, Z. Luo and K. Cen, *J. Anal. Appl. Pyrolysis*, 2008, **82**, 170-177.

85. R. Lou, S. B. Wu and G. J. Lv, *J. Anal. Appl. Pyrolysis*, 2010, **89**, 191-196.

86. G. Jiang, D. J. Nowakowski and A. V. Bridgwater, *Thermochim. Acta*, 2010, **498**, 61-66.

87. D. K. Shen, S. Gu, K. H. Luo, S. R. Wang and M. X. Fang, *Bioresour. Technol.*, 2010, **101**, 6136-6146.

88. M. Asmadi, H. Kawamoto and S. Saka, *J. Anal. Appl. Pyrolysis*, 2011, **92**, 417-425.

89. M. P. Pandey and C. S. Kim, *Chem. Eng. Technol.*, 2011, **34**, 29-41.

90. M. Zhang, F. L. P. Resende, A. Moutsoglou and D. E. Raynie, *J. Anal. Appl. Pyrolysis*, 2012, **98**, 65-71.

91. T. Yoshikawa, T. Yagi, S. Shinohara, T. Fukunaga, Y. Nakasaka, T. Tago and T. Masuda, *Fuel Process. Technol.*, 2013, **108**, 69-75.

92. P. T. Williams and S. Besler, *Fuel*, 1993, **72**, 151-159.

93. T. R. Nunn, J. B. Howard, J. P. Longwell and W. A. Peters, *Ind. Eng. Chem. Proc. Des. Dev.*, 1985, **24**, 836-844.

94. F. Shafizadeh and Y. Z. Lai, *The Journal of Organic Chemistry*, 1972, **37**, 278-284.

95. G. Varhegyi, M. J. Antal, T. Szekely, F. Till and E. Jakab, *Energ. Fuel*, 1988, **2**, 267-272.

96.   O. Boutin, M. Ferrer and J. Lédé, *J. Anal. Appl. Pyrolysis*, 1998, **47**, 13-31.

97.   Y. Liao, S. Wang and X. Ma, *Preprint Papers—American Chemical Society. Division of Fuel Chemistry*, 2004, **49**, 407-411.

98.   H. Kawamoto, H. Morisaki and S. Saka, *J. Anal. Appl. Pyrolysis*, 2009, **85**, 247-251.

99.   S. Cooley and M. J. Antal Jr, *J. Anal. Appl. Pyrolysis*, 1988, **14**, 149-161.

100.   J. B. Berkowitz-Mattuck and T. Noguchi, *J. Appl. Polym. Sci.*, 1963, **7**, 709-725.

101.   J. B. Paine Iii, Y. B. Pithawalla and J. D. Naworal, *J. Anal. Appl. Pyrolysis*, 2008, **83**, 37-63.

102.   J. B. Paine Iii, Y. B. Pithawalla and J. D. Naworal, *J. Anal. Appl. Pyrolysis*, 2008, **82**, 42-69.

103.   J. B. Paine Iii, Y. B. Pithawalla and J. D. Naworal, *J. Anal. Appl. Pyrolysis*, 2008, **82**, 10-41.

104.   G. N. Richards, *J. Anal. Appl. Pyrolysis*, 1987, **10**, 251-255.

105.   G. R. Ponder and G. N. Richards, *Carbohydr. Res.*, 1993, **244**, 27-47.

106.   G. R. Ponder, G. N. Richards and T. T. Stevenson, *J. Anal. Appl. Pyrolysis*, 1992, **22**, 217-229.

107.   D. Shen, R. Xiao, S. Gu and K. Luo, *RSC Advances*, 2011, **1**, 1641-1660.

108.   R. Vinu and L. J. Broadbelt, *Energ. Environ. Sci.*, 2012, **5**, 9808-9826.

109.   P. R. Patwardhan, J. A. Satrio, R. C. Brown and B. H. Shanks, *J. Anal. Appl. Pyrolysis*, 2009, **86**, 323-330.

110.   X. Bai, P. Johnston, S. Sadula and R. C. Brown, *J. Anal. Appl. Pyrolysis*, 2013, **99**, 58-65.

111.   H. Kawamoto, M. Murayama and S. Saka, *Journal of Wood Science*, 2003, **49**, 469-473.

112.   G. A. Byrne, D. Gardiner and F. H. Holmes, *Journal of Applied Chemistry*, 1966, **16**, 81-88.

113.   H. Kawamoto, W. Hatanaka and S. Saka, *J. Anal. Appl. Pyrolysis*, 2003, **70**, 303-313.

114.   M. J. Antal, Jr. and G. Varhegyi, *Ind. Eng. Chem. Res.*, 1995, **34**, 703-717.

115.   S. Yaman, *Energy Convers. Manage.*, 2004, **45**, 651-671.

116.   O. Beaumont, *Wood Fiber Sci.*, 1985, **17**, 228-239.

117.   G. R. Ponder and G. N. Richards, *Carbohydr. Res.*, 1991, **218**, 143-155.

118.   S. Saka and D. A. I. Goring, *Holzforschung*, 1988, **42**, 149-153.

119.   S. Camarero, P. Bocchini, G. C. Galletti and A. T. Martínez, *Rapid Commun. Mass Spectrom.*, 1999, **13**, 630-636.

120.   T.-F. Yeh, B. Goldfarb, H.-m. Chang, I. Peszlen, L. Braun Jennifer and F. Kadla John, *Holzforschung*, 2005, **59**, 669-674.

121.   F. S. Chakar and A. J. Ragauskas, *Industrial Crops and Products*, 2004, **20**, 131-141.

122.   B.-h. Hwang and J. R. Obst, the IAWPS 2003 International Conference on Forest Products: Better Utilization of Wood for Human, Earth and Future, Daejeon, Korea, 2003.

123.   F. J. Ruiz-Dueñas and Á. T. Martínez, *Microbial Biotechnology*, 2009, **2**, 164-177.

124.   S. Chu, A. V. Subrahmanyam and G. W. Huber, *Green Chem.*, 2013, **15**, 125-136.

125.   H. Wenzl, *The chemical technology of wood*, Academic Press, Inc., New York, 1970.

126.   A. J. Stamm, *Industrial & Engineering Chemistry*, 1956, **48**, 413-417.

127.   E. Jakab, K. Liu and H. L. C. Meuzelaar, *Ind. Eng. Chem. Res.*, 1997, **36**, 2087-2095.

128.   D. Meier, J. Berns, C. Grünwald and O. Faix, *J. Anal. Appl. Pyrolysis*, 1993, **25**, 335-347.

129.   J. Dilcio Rocha, C. A. Luengo and C. E. Snape, *Org. Geochem.*, 1999, **30**, 1527-1534.

130.   S. Meesuk, J.-P. Cao, K. Sato, Y. Ogawa and T. Takarada, *J. Anal. Appl. Pyrolysis*, 2012, **94**, 238-245.

131.   D. C. Dayton, J. Carpenter, J. Farmer, B. S. Turk and R. Gupta, *Energ. Fuel*, 2013.

132.   G. Wang, W. Li, B. Li and H. Chen, *Fuel*, 2008, **87**, 552-558.

133.   H. Zhang, R. Xiao, D. Wang, G. He, S. Shao, J. Zhang and Z. Zhong, *Bioresour. Technol.*, 2011,

102, 4258-4264.

134.   R. Zanzi, X. Bai, P. Capdevila and E. Bjornbom, 6th World Congress of Chemical Engineering Melbourne, Australia, 2001.

135.   E. P. Önal, B. B. Uzun and A. E. Pütün, *Fuel Process. Technol.*, 2011, **92**, 879-885.

136.   E. Pütün, F. Ateş and A. E. Pütün, *Fuel*, 2008, **87**, 815-824.

137.   F. Ateş, A. E. Pütün and E. Pütün, *J. Anal. Appl. Pyrolysis*, 2005, **73**, 299-304.

138.   J. D. Adjaye, R. K. Sharma and N. N. Bakhshi, in *Stud. Surf. Sci. Catal.*, eds. J. S. Kevin and C. S. Emerson, Elsevier, 1992, vol. 73, pp. 301-308.

139.   V. Minkova, M. Razvigorova, E. Bjornbom, R. Zanzi, T. Budinova and N. Petrov, *Fuel Process. Technol.*, 2001, **70**, 53-61.

140.   A. Campanella and M. P. Harold, *Biomass Bioenergy*, 2012, **46**, 218-232.

141.   H. Liao, B. Li and B. Zhang, *Journal of Fuel Chemistry and Technology*, 1999, **27**, 268-272.

142.   H. Liao, B. Li and B. Zhang, *Fuel*, 1998, **77**, 847-851.

143.   S. R. A. Kersten, W. P. M. van Swaaij, L. Lefferts and K. Seshan, in *Catalysis for Renewables*, Wiley-VCH Verlag GmbH & Co. KGaA, 2007, pp. 119-145.

144.   J. Lee, Y. Xu and G. W. Huber, *Appl. Catal., B*, 2013, **140-141**, 98-107.

145.   H. Ben, W. Mu, Y. Deng and A. J. Ragauskas, *Fuel*, 2013, **103**, 1148-1153.

146.   G. W. Huber and J. A. Dumesic, *Catal. Today*, 2006, **111**, 119-132.

147.   M. Biddy, A. Dutta, S. Jones and A. Meyer, *Ex-situ catalytic fast pyrolysis technology pathway*, National Renewable Energy Laboratory & Pacific Northwest National Laboratory, 2013.

148.   P. S. Rezaei, H. Shafaghat and W. M. A. W. Daud, *Appl. Catal., A*, 2013.

149.   M. Al-Sabawi, J. Chen and S. Ng, *Energ. Fuel*, 2012, **26**, 5355-5372.

150.   R. Sadeghbeigi, *Fluid Catalytic Cracking Handbook: An Expert Guide to the Practical Operation, Design, and Optimization of FCC Units*, 2nd edn., Gulf Publishing Company, Houston, 2000.

151.   A. Corma, G. W. Huber, L. Sauvanaud and P. O'Connor, *J. Catal.*, 2007, **247**, 307-327.

152.   C. D. Chang and A. J. Silvestri, *J. Catal.*, 1977, **47**, 249-259.

153.   R. Olcese, M. M. Bettahar, B. Malaman, J. Ghanbaja, L. Tibavizco, D. Petitjean and A. Dufour, *Appl. Catal., B*, 2013, **129**, 528-538.

154.   J. Huang, X. Li, D. Wu, H. Tong and W. Li, *Journal of Renewable and Sustainable Energy*, 2013, **5**, -.

155.   J. D. Adjaye and N. N. Bakhshi, *Fuel Process. Technol.*, 1995, **45**, 161-183.

156.   T. R. Carlson, J. Jae, Y.-C. Lin, G. A. Tompsett and G. W. Huber, *J. Catal.*, 2010, **270**, 110-124.

157.   R. Johansson, S. Hruby, J. Rass-Hansen and C. Christensen, *Catal. Lett.*, 2009, **127**, 1-6.

158.   J. Sun and Y. Wang, *Acs Catal.*, 2014, **4**, 1078-1090.

159.   J. F. Haw, W. Song, D. M. Marcus and J. B. Nicholas, *Acc. Chem. Res.*, 2003, **36**, 317-326.

160.   J. L. White, *Catal. Sci. Technol.*, 2011, **1**, 1630-1635.

161.   U. V. Mentzel, S. Shunmugavel, S. L. Hruby, C. H. Christensen and M. S. Holm, *J. Am. Chem. Soc.*, 2009, **131**, 17009-17013.

162.   P. S. Yarlagadda, Y. Hu and N. N. Bakhshi, *Industrial & Engineering Chemistry Product Research and Development*, 1986, **25**, 251-257.

163.   C. Liu, A. M. Karim, V. M. Lebarbier, D. Mei and Y. Wang, *Top. Catal.*, 2013, **56**, 1782-1789.

164.   C. A. Gaertner, J. C. Serrano-Ruiz, D. J. Braden and J. A. Dumesic, *Ind. Eng. Chem. Res.*, 2010, **49**, 6027-6033.

165.   C. A. Gärtner, J. C. Serrano-Ruiz, D. J. Braden and J. A. Dumesic, *ChemSusChem*, 2009, **2**,

1121-1124.

166.   C. A. Gaertner, J. C. Serrano-Ruiz, D. J. Braden and J. A. Dumesic, *J. Catal.*, 2009, **266**, 71-78.

167.   C. J. Barrett, J. N. Chheda, G. W. Huber and J. A. Dumesic, *Appl. Catal., B*, 2006, **66**, 111-118.

168.   A. Gangadharan, M. Shen, T. Sooknoi, D. E. Resasco and R. G. Mallinson, *Appl. Catal., A*, 2010, **385**, 80-91.

169.   E. I. Gurbuz, E. L. Kunkes and J. A. Dumesic, *Green Chem.*, 2010, **12**, 223-227.

170.   R. W. Snell, E. Combs and B. H. Shanks, *Top. Catal.*, 2010, **53**, 1248-1253.

171.   R. Klimkiewicz, E. Fabisz, I. Morawski, H. Grabowska and L. Syper, *Journal of Chemical Technology & Biotechnology*, 2001, **76**, 35-38.

172.   M. Glinski, W. Szymanski and D. Lomot, *Appl. Catal., A*, 2005, **281**, 107-113.

173.   M. Gliński, J. Kijeński and A. Jakubowski, *Appl. Catal., A*, 1995, **128**, 209-217.

174.   A. A. Taimoor, A. Favre-Reguillon, L. Vanoye and I. Pitault, *Catal. Sci. Technol.*, 2012, **2**, 359-363.

175.   W. H. Brown, B. L. Iverson, E. V. Anslyn and C. S. Foote, *Organic chemistry seventh edition*, Brooks/Cole, Belmont CA, 2013.

176.   Y.-C. Chang and A.-N. Ko, *Appl. Catal., A*, 2000, **190**, 149-155.

177.   G. Zhang, H. Hattori and K. Tanabe, *Appl. Catal.*, 1988, **36**, 189-197.

178.   S. Lippert, W. Baumann and K. Thomke, *J. Mol. Catal.*, 1991, **69**, 199-214.

179.   W. Ji, Y. Chen and H. H. Kung, *Appl. Catal., A*, 1997, **161**, 93-104.

180.   W. J. Ji and Y. Chen, *Chemical Journal of Chinese Universities-Chinese*, 1997, **18**, 277-280.

181.   M. T. Casale, A. R. Richman, M. J. Elrod, R. M. Garland, M. R. Beaver and M. A. Tolbert, *Atmos. Environ.*, 2007, **41**, 6212-6224.

182.   E. Laurent and B. Delmon, *Appl. Catal., A*, 1994, **109**, 77-96.

183.   E. Furimsky, *Catalysis reviews*, 1983, **25**, 421-458.

184.   E. Furimsky, *Appl. Catal., A*, 2000, **199**, 147-190.

185.   E. Furimsky, *Catal. Today*, 2013, **217**, 13-56.

186.   D. C. Elliott and T. R. Hart, *Energ. Fuel*, 2009, **23**, 631-637.

187.   E. Laurent and B. Delmon, *Appl. Catal., A*, 1994, **109**, 97-115.

188.   M. A. n. González-Borja and D. E. Resasco, *Energ. Fuel*, 2011, **25**, 4155-4162.

189.   T. Nimmanwudipong, R. C. Runnebaum, D. E. Block and B. C. Gates, *Energ. Fuel*, 2011, **25**, 3417-3427.

190.   X. Zhu, L. L. Lobban, R. G. Mallinson and D. E. Resasco, *J. Catal.*, 2011, **281**, 21-29.

191.   P. T. M. Do, A. J. Foster, J. Chen and R. F. Lobo, *Green Chem.*, 2012, **14**, 1388-1397.

192.   T. Nimmanwudipong, C. Aydin, J. Lu, R. Runnebaum, K. Brodwater, N. Browning, D. Block and B. Gates, *Catal. Lett.*, 2012, **142**, 1190-1196.

193.   J. Sun, A. M. Karim, H. Zhang, L. Kovarik, X. S. Li, A. J. Hensley, J.-S. McEwen and Y. Wang, *J. Catal.*, 2013, **306**, 47-57.

194.   S. Sitthisa and D. E. Resasco, *Catal. Lett.*, 2011, **141**, 784-791.

195.   M. A. Alotaibi, E. F. Kozhevnikova and I. V. Kozhevnikov, *Appl. Catal., A*, 2012, **447–448**, 32-40.

196.   S. Leng, X. Wang, X. He, L. Liu, Y. e. Liu, X. Zhong, G. Zhuang and J.-g. Wang, *Catal. Commun.*, 2013, **41**, 34-37.

197.   D. Wang, D. Montané and E. Chornet, *Appl. Catal., A*, 1996, **143**, 245-270.

198.   D. Wang, S. Czernik, D. Montané, M. Mann and E. Chornet, *Ind. Eng. Chem. Res.*, 1997, **36**, 1507-1518.

199. D. Wang, S. Czernik and E. Chornet, *Energ. Fuel*, 1998, **12**, 19-24.
200. R. Trane, S. Dahl, M. S. Skjøth-Rasmussen and A. D. Jensen, *Int. J. Hydrog. Energy*, 2012, **37**, 6447-6472.
201. S. Czernik, R. French, C. Feik and E. Chornet, 1999, 827-832.
202. M. Marquevich, S. Czernik, E. Chornet and D. Montané, *Energ. Fuel*, 1999, **13**, 1160-1166.
203. Z. Wang, Y. Pan, T. Dong, X. Zhu, T. Kan, L. Yuan, Y. Torimoto, M. Sadakata and Q. Li, *Appl. Catal., A*, 2007, **320**, 24-34.
204. J. Sun, D. Mei, A. M. Karim, A. K. Datye and Y. Wang, *ChemCatChem*, 2013, **5**, 1299-1303.
205. P. J. Ortiz-Toral, J. Satrio, R. C. Brown and B. H. Shanks, *Energ. Fuel*, 2011, **25**, 3289-3297.
206. M. C. Samolada, A. Papafotica and I. A. Vasalos, *Energ. Fuel*, 2000, **14**, 1161-1167.
207. T. R. Carlson, T. P. Vispute and G. W. Huber, *ChemSusChem*, 2008, **1**, 397-400.
208. E. Pütün, B. B. Uzun and A. E. Pütün, *Energ. Fuel*, 2009, **23**, 2248-2258.
209. A. Pattiya, J. O. Titiloye and A. V. Bridgwater, *Fuel*, 2010, **89**, 244-253.
210. Q. Lu, X. Zhu, W. Li, Y. Zhang and D. Chen, *Chin. Sci. Bull.*, 2009, **54**, 1941-1948.
211. M. Q. Chen, J. Wang, M. X. Zhang, M. G. Chen, X. F. Zhu, F. F. Min and Z. C. Tan, *J. Anal. Appl. Pyrolysis*, 2008, **82**, 145-150.
212. S. D. Stefanidis, K. G. Kalogiannis, E. F. Iliopoulou, A. A. Lappas and P. A. Pilavachi, *Bioresour. Technol.*, 2011, **102**, 8261-8267.
213. Q. Lu, Z. F. Zhang, C. Q. Dong and X. F. Zhu, *Energies*, 2010, **3**, 1805-1820.
214. F. A. Agblevor and S. Besler, *Energ. Fuel*, 1996, **10**, 293-298.
215. A. Jensen, K. Dam-Johansen, M. A. Wójtowicz and M. A. Serio, *Energ. Fuel*, 1998, **12**, 929-938.
216. D. J. Nowakowski, C. R. Woodbridge and J. M. Jones, *J. Anal. Appl. Pyrolysis*, 2008, **83**, 197-204.
217. F. Shafizadeh, *J. Anal. Appl. Pyrolysis*, 1982, **3**, 283-305.
218. R. Fahmi, A. V. Bridgwater, I. Donnison, N. Yates and J. M. Jones, *Fuel*, 2008, **87**, 1230-1240.
219. K. Raveendran, A. Ganesh and K. C. Khilar, *Fuel*, 1995, **74**, 1812-1822.
220. C. A. Zaror, I. S. Hutchings, D. L. Pyle, H. N. Stiles and R. Kandiyoti, *Fuel*, 1985, **64**, 990-994.
221. L. Zhou, Y. Jia, T.-H. Nguyen, A. A. Adesina and Z. Liu, *Fuel Process. Technol.*, 2013, **116**, 149-157.
222. W.-P. Pan and G. N. Richards, *J. Anal. Appl. Pyrolysis*, 1989, **16**, 117-126.
223. G. Varhegyi, M. J. Antal, T. Szekely, F. Till, E. Jakab and P. Szabo, *Energ. Fuel*, 1988, **2**, 273-277.
224. G. N. Richards, F. Shafizadeh and T. T. Stevenson, *Carbohydr. Res.*, 1983, **117**, 322-327.
225. M. Kleen and G. Gellerstedt, *J. Anal. Appl. Pyrolysis*, 1995, **35**, 15-41.
226. G. N. Richards and G. Zheng, *J. Anal. Appl. Pyrolysis*, 1991, **21**, 133-146.
227. Q. Lu, Z. Wang, C. Q. Dong, Z. F. Zhang, Y. Zhang, Y. P. Yang and X. F. Zhu, *J. Anal. Appl. Pyrolysis*, 2011, **91**, 273-279.
228. N. Shimada, H. Kawamoto and S. Saka, *J. Anal. Appl. Pyrolysis*, 2008, **81**, 80-87.
229. P. R. Patwardhan, J. A. Satrio, R. C. Brown and B. H. Shanks, *Bioresour. Technol.*, 2010, **101**, 4646-4655.
230. I.-Y. Eom, J.-Y. Kim, S.-M. Lee, T.-S. Cho, H. Yeo and J.-W. Choi, *Bioresour. Technol.*, 2013, **128**, 664-672.
231. W. K. Tang, *Effect of inorganic salts on pyrolysis of wood, alpha-cellulose, and lignin determined by dynamic thermogravimetry*, DTIC Document, 1967.
232. W. K. Tang and H. W. Eickner, *Effect of inorganic salts on pyrolysis of wood, cellulose, and*

lignin determined by differential thermal analysis, DTIC Document, 1968.

233. S. D. Jackson and J. S. Hargreaves, *Metal oxide catalysis*, Wiley Online Library, 2009.
234. J. L. G. Fierro, *Metal Oxides: chemistry and applications*, CRC press, 2006.
235. I. E. Wachs, *Catal. Today*, 2005, **100**, 79-94.
236. D. Fabbri, C. Torri and V. Baravelli, *J. Anal. Appl. Pyrolysis*, 2007, **80**, 24-29.
237. T. Mochizuki, D. Atong, S.-Y. Chen, M. Toba and Y. Yoshimura, *Catal. Commun.*, 2013, **36**, 1-4.
238. Q. Lu, W.-M. Xiong, W.-Z. Li, Q.-X. Guo and X.-F. Zhu, *Bioresour. Technol.*, 2009, **100**, 4871-4876.
239. Z. Wang, Q. Lu, X.-F. Zhu and Y. Zhang, *ChemSusChem*, 2011, **4**, 79-84.
240. E. Pütün, *Energy*, 2010, **35**, 2761-2766.
241. L. Zhou, H. Yang, H. Wu, M. Wang and D. Cheng, *Fuel Process. Technol.*, 2013, **106**, 385-391.
242. L. Deng, Y. Fu and Q.-X. Guo, *Energ. Fuel*, 2008, **23**, 564-568.
243. W.-L. Fanchiang and Y.-C. Lin, *Appl. Catal., A*, 2012, **419–420**, 102-110.
244. C. Liu, J. Sun, C. Smith and Y. Wang, *Appl. Catal., A*, 2013, **467**, 91-97.
245. J. Sun, K. Zhu, F. Gao, C. Wang, J. Liu, C. H. F. Peden and Y. Wang, *J. Am. Chem. Soc.*, 2011, **133**, 11096-11099.
246. J. Jae, G. A. Tompsett, A. J. Foster, K. D. Hammond, S. M. Auerbach, R. F. Lobo and G. W. Huber, *J. Catal.*, 2011, **279**, 257-268.
247. K. Murata, Y. Liu, M. Inaba and I. Takahara, *J. Anal. Appl. Pyrolysis*, 2012, **94**, 75-82.
248. T. F. Degnan, G. K. Chitnis and P. H. Schipper, *Microporous Mesoporous Mater.*, 2000, **35–36**, 245-252.
249. D. J. Mihalcik, C. A. Mullen and A. A. Boateng, *J. Anal. Appl. Pyrolysis*, 2011, **92**, 224-232.
250. M. A. Jackson, D. L. Compton and A. A. Boateng, *J. Anal. Appl. Pyrolysis*, 2009, **85**, 226-230.
251. S. Vitolo, M. Seggiani, P. Frediani, G. Ambrosini and L. Politi, *Fuel*, 1999, **78**, 1147-1159.
252. R. K. Sharma and N. N. Bakhshi, *Bioresour. Technol.*, 1993, **45**, 195-203.
253. R. K. Sharma and N. N. Bakhshi, *Fuel Process. Technol.*, 1993, **35**, 201-218.
254. R. K. Sharma and N. N. Bakhshi, *Biomass Bioenergy*, 1993, **5**, 445-455.
255. J. D. Adjaye and N. N. Bakhshi, *Fuel Process. Technol.*, 1995, **45**, 185-202.
256. J. D. Adjaye and N. N. Bakhshi, *Biomass Bioenergy*, 1995, **8**, 131-149.
257. P. T. Williams and N. Nugranad, *Energy*, 2000, **25**, 493-513.
258. P. T. Williams and P. A. Horne, *Fuel*, 1995, **74**, 1839-1851.
259. H. Zhang, R. Xiao, H. Huang and G. Xiao, *Bioresour. Technol.*, 2009, **100**, 1428-1434.
260. A. G. Gayubo, A. T. Aguayo, A. Atutxa, R. Aguado and J. Bilbao, *Ind. Eng. Chem. Res.*, 2004, **43**, 2610-2618.
261. A. G. Gayubo, A. T. Aguayo, A. Atutxa, R. Aguado, M. Olazar and J. Bilbao, *Ind. Eng. Chem. Res.*, 2004, **43**, 2619-2626.
262. A. G. Gayubo, A. T. Aguayo, A. Atutxa, R. Prieto and J. Bilbao, *Energ. Fuel*, 2004, **18**, 1640-1647.
263. T. Q. Hoang, X. Zhu, T. Sooknoi, D. E. Resasco and R. G. Mallinson, *J. Catal.*, 2010, **271**, 201-208.
264. U. V. Mentzel and M. S. Holm, *Appl. Catal., A*, 2011, **396**, 59-67.
265. Y. Zhao, T. Pan, Y. Zuo, Q.-X. Guo and Y. Fu, *Bioresour. Technol.*, 2013, **147**, 37-42.
266. I. Graça, J. M. Lopes, M. F. Ribeiro, F. Ramôa Ribeiro, H. S. Cerqueira and M. B. B. de Almeida, *Appl. Catal., B*, 2011, **101**, 613-621.

46

267. Z. Ma, E. Troussard and J. A. van Bokhoven, *Appl. Catal., A*, 2012, **423–424**, 130-136.

268. C. A. Mullen and A. A. Boateng, *Fuel Process. Technol.*, 2010, **91**, 1446-1458.

269. Y. Yu, X. Li, L. Su, Y. Zhang, Y. Wang and H. Zhang, *Appl. Catal., A*, 2012, **447–448**, 115-123.

270. S. Vitolo, B. Bresci, M. Seggiani and M. G. Gallo, *Fuel*, 2001, **80**, 17-26.

271. J. Sun and Y. Wang, *Acs Catal.*, 2014, **DOI:** 10.1021/cs4011343.

272. F. A. Twaiq, N. A. M. Zabidi and S. Bhatia, *Ind. Eng. Chem. Res.*, 1999, **38**, 3230-3237.

273. X. Li, L. Su, Y. Wang, Y. Yu, C. Wang, X. Li and Z. Wang, *Frontiers of Environmental Science & Engineering*, 2012, **6**, 295-303.

274. A. J. Foster, J. Jae, Y.-T. Cheng, G. W. Huber and R. F. Lobo, *Appl. Catal., A*, 2012, **423–424**, 154-161.

275. K. V. Padmaja, N. Atheya and A. K. Bhatnagar, *Biomass & Bioenergy*, 2009, **33**, 1664-1669.

276. O. D. Mante, F. A. Agblevor and R. McClung, *Fuel*, 2013, **108**, 451-464.

277. P. A. Horne and P. T. Williams, *Fuel*, 1996, **75**, 1043-1050.

278. T. R. Carlson, Y.-T. Cheng, J. Jae and G. W. Huber, *Energ. Environ. Sci.*, 2011, **4**, 145-161.

279. A. Atutxa, R. Aguado, A. G. Gayubo, M. Olazar and J. Bilbao, *Energ. Fuel*, 2005, **19**, 765-774.

280. A. G. Gayubo, B. Valle, A. s. T. Aguayo, M. n. Olazar and J. Bilbao, *Energ. Fuel*, 2009, **23**, 4129-4136.

281. P. A. Horne, N. Nugranad and P. T. Williams, *J. Anal. Appl. Pyrolysis*, 1995, **34**, 87-108.

282. B. Valle, A. G. Gayubo, A. s. T. Aguayo, M. Olazar and J. Bilbao, *Energ. Fuel*, 2010, **24**, 2060-2070.

283. X. Li, H. Zhang, J. Li, L. Su, J. Zuo, S. Komarneni and Y. Wang, *Appl. Catal., A*, 2013, **455**, 114-121.

284. H. Zhang, Y.-T. Cheng, T. P. Vispute, R. Xiao and G. W. Huber, *Energ. Environ. Sci.*, 2011, **4**, 2297-2307.

285. H. Zhang, T. R. Carlson, R. Xiao and G. W. Huber, *Green Chem.*, 2012, **14**, 98-110.

286. F. Melligan, M. H. B. Hayes, W. Kwapinski and J. J. Leahy, *Energ. Fuel*, 2012, **26**, 6080-6090.

287. S. Thangalazhy-Gopakumar, S. Adhikari and R. B. Gupta, *Energ. Fuel*, 2012, **26**, 5300-5306.

288. I. s. Graça, J.-D. Comparot, S. b. Laforge, P. Magnoux, J. M. Lopes, M. F. Ribeiro and F. Ramôa Ribeiro, *Energ. Fuel*, 2009, **23**, 4224-4230.

289. R. K. Sharma and N. N. Bakhshi, *Energ. Fuel*, 1993, **7**, 306-314.

290. A. G. Gayubo, A. T. Aguayo, A. Atutxa, R. Prieto and J. Bilbao, *Ind. Eng. Chem. Res.*, 2004, **43**, 5042-5048.

291. R. French and S. Czernik, *Fuel Process. Technol.*, 2010, **91**, 25-32.

292. H. Ju Park, Y.-K. Park, J.-S. Kim, J.-K. Jeon, K.-S. Yoo, J.-H. Yim, J. Jung and J. Min Sohn, in *Stud. Surf. Sci. Catal.*, eds. I.-S. N. Hyun-Ku Rhee and P. Jong Moon, Elsevier, 2006, vol. Volume 159, pp. 553-556.

293. Y.-T. Cheng, Z. Wang, C. J. Gilbert, W. Fan and G. W. Huber, *Angew. Chem. Int. Ed.*, 2012, **51**, 11097-11100.

294. E. F. Iliopoulou, S. D. Stefanidis, K. G. Kalogiannis, A. Delimitis, A. A. Lappas and K. S. Triantafyllidis, *Appl. Catal., B*, 2012, **127**, 281-290.

295. G. Neumann and J. Hicks, *Top. Catal.*, 2012, **55**, 196-208.

296. Y. Yang, C. Sun, J. Du, Y. Yue, W. Hua, C. Zhang, W. Shen and H. Xu, *Catal. Commun.*, 2012, **24**, 44-47.

297. C. Hong, F. Gong, M. Fan, Q. Zhai, W. Huang, T. Wang and Q. Li, *Journal of Chemical*

Technology & Biotechnology, 2013, **88**, 109-118.

298. Y. K. Ong and S. Bhatia, *Energy*, 2010, **35**, 111-119.

299. J. D. Adjaye and N. N. Bakhshi, *Biomass Bioenergy*, 1994, **7**, 201-211.

300. A. Aho, N. Kumar, K. Eränen, T. Salmi, M. Hupa and D. Y. Murzin, *Fuel*, 2008, **87**, 2493-2501.

301. H. Ben and A. J. Ragauskas, *RSC Advances*, 2012, **2**, 12892-12898.

302. J. Huang, W. Long, P. K. Agrawal and C. W. Jones, *J. Phys. Chem. C*, 2009, **113**, 16702-16710.

303. B. B. Uzun and N. Sarioğlu, *Fuel Process. Technol.*, 2009, **90**, 705-716.

304. A. Aho, N. Kumar, A. V. Lashkul, K. Eränen, M. Ziolek, P. Decyk, T. Salmi, B. Holmbom, M. Hupa and D. Y. Murzin, *Fuel*, 2010, **89**, 1992-2000.

305. A. Aho, A. Tokarev, P. Backman, N. Kumar, K. Eränen, M. Hupa, B. Holmbom, T. Salmi and D. Y. Murzin, *Top. Catal.*, 2011, **54**, 941-948.

306. A. Aho, N. Kumar, K. Eränen, T. Salmi, M. Hupa and D. Y. Murzin, *Process Saf. Environ. Prot.*, 2007, **85**, 473-480.

307. N. Taufiqurrahmi and S. Bhatia, *Energ. Environ. Sci.*, 2011, **4**, 1087-1112.

308. T. Mochizuki, M. Toba and Y. Yoshimura, *J. Jpn. Pet. Inst.*, 2012, **55**, 69-70.

309. A. Marcilla, M. I. Beltrán, F. Hernández and R. Navarro, *Appl. Catal., A*, 2004, **278**, 37-43.

310. F. A. Twaiq, A. R. Mohamed and S. Bhatia, *Microporous Mesoporous Mater.*, 2003, **64**, 95-107.

311. F. A. Twaiq, N. A. M. Zabidi, A. R. Mohamed and S. Bhatia, *Fuel Process. Technol.*, 2003, **84**, 105-120.

312. E. F. Iliopoulou, E. V. Antonakou, S. A. Karakoulia, I. A. Vasalos, A. A. Lappas and K. S. Triantafyllidis, *Chem. Eng. J.*, 2007, **134**, 51-57.

313. J. Adam, M. Blazsó, E. Mészáros, M. Stöcker, M. H. Nilsen, A. Bouzga, J. E. Hustad, M. Grønli and G. Øye, *Fuel*, 2005, **84**, 1494-1502.

314. E. Antonakou, A. Lappas, M. H. Nilsen, A. Bouzga and M. Stöcker, *Fuel*, 2006, **85**, 2202-2212.

315. S. Stephanidis, C. Nitsos, K. Kalogiannis, E. F. Iliopoulou, A. A. Lappas and K. S. Triantafyllidis, *Catal. Today*, 2011, **167**, 37-45.

316. M. H. Nilsen, E. Antonakou, A. Bouzga, A. Lappas, K. Mathisen and M. Stöcker, *Microporous Mesoporous Mater.*, 2007, **105**, 189-203.

317. J. M. Sun and X. H. Bao, *Chemistry-a European Journal*, 2008, **14**, 7478-7488.

318. Q. Lu, W.-z. Li, D. Zhang and X.-f. Zhu, *J. Anal. Appl. Pyrolysis*, 2009, **84**, 131-138.

319. J. Adam, E. Antonakou, A. Lappas, M. Stöcker, M. H. Nilsen, A. Bouzga, J. E. Hustad and G. Øye, *Microporous Mesoporous Mater.*, 2006, **96**, 93-101.

320. K. S. Triantafyllidis, E. F. Iliopoulou, E. V. Antonakou, A. A. Lappas, H. Wang and T. J. Pinnavaia, *Microporous Mesoporous Mater.*, 2007, **99**, 132-139.

321. H. J. Park, K.-H. Park, J.-K. Jeon, J. Kim, R. Ryoo, K.-E. Jeong, S. H. Park and Y.-K. Park, *Fuel*, 2012, **97**, 379-384.

322. F. de Miguel Mercader, M. J. Groeneveld, S. R. A. Kersten, N. W. J. Way, C. J. Schaverien and J. A. Hogendoorn, *Appl. Catal., B*, 2010, **96**, 57-66.

323. D. C. Elliott, T. R. Hart, G. G. Neuenschwander, L. J. Rotness and A. H. Zacher, *Environmental Progress & Sustainable Energy*, 2009, **28**, 441-449.

324. R. H. Venderbosch, A. R. Ardiyanti, J. Wildschut, A. Oasmaa and H. J. Heeres, *Journal of Chemical Technology & Biotechnology*, 2010, **85**, 674-686.

325. G. W. Huber and A. Corma, *Angew. Chem. Int. Ed.*, 2007, **46**, 7184-7201.

326. M. A. Alotaibi, E. F. Kozhevnikova and I. V. Kozhevnikov, *J. Catal.*, 2012, **293**, 141-144.

327. E. L. Kunkes, E. I. Gurbuz and J. A. Dumesic, *J. Catal.*, 2009, **266**, 236-249.

328. S. Sitthisa, T. Pham, T. Prasomsri, T. Sooknoi, R. G. Mallinson and D. E. Resasco, *J. Catal.*, 2011, **280**, 17-27.

329. Q. Lu, Z. Tang, Y. Zhang and X. F. Zhu, *Ind. Eng. Chem. Res.*, 2010, **49**, 2573-2580.

330. E.-J. Shin and M. A. Keane, *Ind. Eng. Chem. Res.*, 2000, **39**, 883-892.

331. V. Vorotnikov, G. Mpourmpakis and D. G. Vlachos, *Acs Catal.*, 2012, **2**, 2496-2504.

332. R. N. Olcese, M. Bettahar, D. Petitjean, B. Malaman, F. Giovanella and A. Dufour, *Appl. Catal., B*, 2012, **115–116**, 63-73.

333. R. Runnebaum, T. Nimmanwudipong, J. Doan, D. Block and B. Gates, *Catal. Lett.*, 2012, **142**, 664-666.

334. T. Nimmanwudipong, R. Runnebaum, D. Block and B. Gates, *Catal. Lett.*, 2011, **141**, 779-783.

335. R. C. Runnebaum, R. J. Lobo-Lapidus, T. Nimmanwudipong, D. E. Block and B. C. Gates, *Energ. Fuel*, 2011, **25**, 4776-4785.

336. R. Runnebaum, T. Nimmanwudipong, D. Block and B. Gates, *Catal. Lett.*, 2011, **141**, 817-820.

337. R. C. Runnebaum, T. Nimmanwudipong, R. R. Limbo, D. E. Block and B. C. Gates, *Catal. Lett.*, 2012, **142**, 7-15.

338. A. J. Foster, P. T. M. Do and R. F. Lobo, *Top. Catal.*, 2012, **55**, 118-128.

339. M. S. Zanuttini, C. D. Lago, C. A. Querini and M. A. Peralta, *Catal. Today*, 2013, **213**, 9-17.

340. H. J. Park, H. S. Heo, J.-K. Jeon, J. Kim, R. Ryoo, K.-E. Jeong and Y.-K. Park, *Appl. Catal., B*, 2010, **95**, 365-373.

341. T. S. Nguyen, M. Zabeti, L. Lefferts, G. Brem and K. Seshan, *Biomass Bioenergy*, 2013, **48**, 100-110.

342. A. Güngör, S. Önenç, S. Uçar and J. Yanik, *J. Anal. Appl. Pyrolysis*, 2012, **97**, 39-48.

343. M. Olazar, R. Aguado, J. Bilbao and A. Barona, *AlChE J.*, 2000, **46**, 1025-1033.

344. T. S. Nguyen, M. Zabeti, L. Lefferts, G. Brem and K. Seshan, *Bioresour. Technol.*, 2013, **142**, 353-360.

345. H. J. Park, J. I. Dong, J. K. Jeon, K. S. Yoo, J. H. Yim, J. M. Sohn and Y. K. Park, *Journal of Industrial and Engineering Chemistry*, 2007, **13**, 182-189.

346. M.-J. Jeon, S.-S. Kim, J.-K. Jeon, S. Park, J. Kim, J. Sohn, S.-H. Lee and Y.-K. Park, *Nanoscale Research Letters*, 2012, **7**, 1-5.

347. H. Zhang, R. Xiao, B. Jin, D. Shen, R. Chen and G. Xiao, *Bioresour. Technol.*, 2013, **137**, 82-87.

348. H. Zhang, R. Xiao, Q. Pan, Q. Song and H. Huang, *Chem. Eng. Technol.*, 2009, **32**, 27-37.

349. A. Aho, N. Kumar, K. Eränen, B. Holmbom, M. Hupa, T. Salmi and D. Murzin, *International Journal of Molecular Sciences*, 2008, **9**, 1665-1675.

350. F. A. Agblevor, S. Beis, O. Mante and N. Abdoulmoumine, *Ind. Eng. Chem. Res.*, 2010, **49**, 3533-3538.

351. C. A. Mullen, A. A. Boateng, D. J. Mihalcik and N. M. Goldberg, *Energ. Fuel*, 2011, **25**, 5444-5451.

352. E. Pütün, B. B. Uzun and A. E. Pütün, *Bioresour. Technol.*, 2006, **97**, 701-710.

353. K. Giannakopoulou, M. Lukas, A. Vasiliev, C. Brunner and H. Schnitzer, *Microporous Mesoporous Mater.*, 2010, **128**, 126-135.

354. S. J. Choi, S. H. Park, J.-K. Jeon, I. G. Lee, C. Ryu, D. J. Suh and Y.-K. Park, *Renewable Energy*, 2013, **54**, 105-110.

355. X. X. Zheng, C. F. Yan, R. R. Hu, J. Li, H. Hai, W. M. Luo, C. Q. Guo, W. B. Li and Z. Y. Zhou, *Int. J.*

Hydrog. Energy, 2012, **37**, 12987-12993.

Graphic Abstract
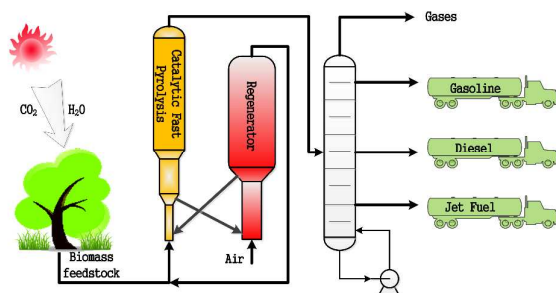
We summarize the development of catalysts and provide current understanding of the chemistry for catalytic fast pyrolysis of lignocelluloses biomass.

Changjun Liu received his PhD in Chemical Engineering from Sichuan University in 2010 (supervised by Prof. Enze Min and Prof. Bin Liang), then worked as a postdoc research associate with Prof. Yong Wang in the Gene & Linda Voiland School of Chemical Engineering and Bioengineering, Washington State University, USA. His current research interests include biomass conversion, bio-oil upgrading, selective hydrogenation, acid-base catalysis, and two-phase flow.

Dr. Huamin Wang is currently a research engineer in Pacific Northwest National Laboratory. He received his Ph.D. from Nankai University, China and then did postdoctoral research in ETH Zurich and UC Berkeley. He has experience in heterogeneous catalysis, inorganic material synthesis, hydroprocessing, and biomass conversion. His current research involves thermochemical conversion of biomass and fundamental understanding of catalytic conversion of oxygenates.


Ayman M. Karim is currently a senior research scientist at Pacific Northwest National Laboratory (PNNL). Prior to joining PNNL he did a postdoctoral stay (2007-2008) with Prof. Dionisios G. Vlachos at the University of Delaware. He obtained his Ph.D. in chemical engineering from the University of New Mexico (2007) under the guidance of Prof. Abhaya K. Datye. His current

research interests include fundamental studies of colloidal nanoparticles synthesis mechanisms, *in situ* and *in operando* catalyst characterization by x-ray absorption spectroscopy and developing novel catalytic materials for the synthesis of fuels and chemicals from biomass.

Junming Sun is an assistant research & major professor in Prof. Yong Wang's group at Washington State University, USA. He received his PhD from Dalian Institute of Chemical Physics of Chinese Academy of Science in 2007 (Prof. Xinhe Bao), after which he worked with Prof. Bruce C. Gates at UC Davis (2007–2008) and then with Prof. Yong Wang at Pacific Northwest National Laboratory (2008–2011) as a postdoc researcher. His current research interests include fundamental understanding and rational design of acid-base/supported metal catalysts for biomass derived small oxygenates, bimetallic catalysis for hydrodeoxygenation.
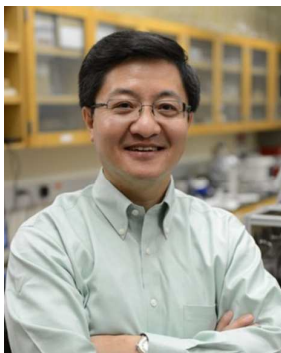
Yong Wang joined Pacific Northwest National Laboratory (PNNL), USA in 1994 and was promoted to Laboratory Fellow in 2005. In 2009, he assumed a joint position at Washington State University (WSU) and PNNL. In this unique position, he continues to be a Laboratory Fellow at PNNL and is the Voiland Distinguished Professor in Chemical Engineering at WSU, a full professorship with tenure. His research interests include the development of novel catalytic materials and reaction engineering for the conversion of fossil and biomass feedstocks to fuels and chemicals